SAND2016-0515R

SANDIA REPORT

SAND200X-XXXX
Unlimited Release
Printed Month and Year

Netflow Theory Manual

Radoslav Bozinoski and William Winters

Prepared by
Sandia National Laboratories
Albuquerque, New Mexico 87185 and Livermore, California 94550

Sandia National Laboratories is a multi-program laboratory managed and operated by Sandia Corporation, a wholly owned subsidiary of Lockheed Martin Corporation, for the U.S. Department of Energy's National Nuclear Security Administration under contract DE-AC04-94AL85000.

Approved for public release; further dissemination unlimited.

Issued by Sandia National Laboratories, operated for the United States Department of Energy by Sandia Corporation.

Available to DOE and DOE contractors from
U.S. Department of Energy
Office of Scientific and Technical Information
P.O. Box 62
Oak Ridge, TN 37831

Telephone: (865) 576-8401
Facsimile: (865) 576-5728
E-Mail: reports@osti.gov
Online ordering: http://www.osti.gov/scitech

Available to the public from
U.S. Department of Commerce
National Technical Information Service
5301 Shawnee Rd
Alexandria, VA 22312

Telephone: (800) 553-6847
Facsimile: (703) 605-6900
E-Mail: orders@ntis.gov
Online order: http://www.ntis.gov/search

SAND200X-XXXX
Unlimited Release
Printed Month Year

Netflow Theory Manual

Radoslav Bozinoski and William Winters
Thermal/Fluids Science & Engineering Org. 8253
Sandia National Laboratories
P.O. Box 5800
Livermore, California 87185-MSXXXX

Abstract

The purpose of this report is to document the theoretical models utilized by the computer code NETFLOW. This report will focus on the theoretical models used to analyze high Mach number fully compressible transonic flows in piping networks.

Table of Contents

NOMENCLATURE

Upper Case

A_J	Cross-sectional flow area of path J
A_N	Cross-sectional flow area of node N
A_S	Wall heat transfer surface area for a node
C	Sound speed, wall specific heat
C_p	Specific heat at constant pressure
C_S	Sound speed
C_v	Specific heat at constant volume
D_h	Hydraulic diameter
E_N	Total energy at a node, $M_N(u_N + v_N^2/2)$
$\dot{E}_n$	Energy generation rate at node N
F	Area ratio as defined in Equation (2.25)
F_i	The i^{th} DASKR residual
J	Integer index attributed to paths
$JMAX$	The maximum J
K	Integer index attributed to species
$KMAX$	The maximum K
K_A	Form loss coefficient due to area transitions
K_f	Form loss coefficient due to wall friction
K_L	User supplied form loss coefficient
L_J	Length of path J
M_a	Mach number

M_N	Mass of the gas mixture in node N
$\dot{M}_N$	Gas mixture mass generation rated in node N
$M_{N,K}$	Mass of species K in node N
N	Integer index attributed to nodes
N_{up}	The node upstream
N_{DN}	The node downstream
Nu	Nusselt number
Nu_L	Laminar Nusselt number
Nu_T	Turbulent Nusselt number
Nu_{forced}	Forced convection Nusselt number
P	Pressure
P_0	Total Pressure
Pr	Prandtl number Equation (4.7), pressure ratio
Pr_{crit}	Critical pressure ration
R	Ideal gas constant
$\bar{R}$	Universal gas constant
Ra	Rayleigh number as defined in Equation (4.11)
Re	Reynolds number as defined in Equation (4.2)
S_J	Sign of the flow in path J
T	Temperature
T_0	Total Temperature
T_N	Temperature of the gas mixture in node N
T_W	The wall surface temperature
T_{AMB}	The ambient temperature
V	Volume

W_J	Mass flow rate in path J
W_N	Mass flow rate in node N
$Y_{N,K}$	The mass fraction of species K in node N
$Y_{J,K}$	The mass fraction of species K in path J
Z	Compressibility factor

Lower Case

a	Thermal diffusivity
b	Abel-Noble co-volume constant
f	Moody friction factor
h	Newton's law of cooling heat transfer coefficient
k	Thermal conductivity
u	Mixture internal energy per unit mass
u_N	Mixture internal energy per unit mass in node N
v	Velocity of gas mixture
v_N	Velocity of gas mixture in node N
y_i	The i^{th} DASKR dependent variable

Greek Symbols

$\alpha_1, \alpha_2, \alpha_3$	Valve empirical constants, Equation (2,21)
β	Volume expansivity, Equation 3.16) and Valve pressure ratio, Equation (2.19)
β_{crit}	Critical valve pressure ratio, Equation (2.20)
δ	Valve parameter defined by Equation (2.23)
ϵ	Wall surface roughness
γ	Ratio of specific heats, Equation (3.14)

μ	Viscosity

Subscripts

N	At node N
J	At path J
NUP	At the upstream node
NDN	At the downstream node
SONIC	The sonic value

INTRODUCTION

The purpose of this report is to document the theoretical models utilized by the computer code NETFLOW. NETFLOW was originally developed to model the transport of contaminants through architectural spaces (office buildings, airport terminals, etc.). Flows through buildings are mainly driven by heating, ventilation and air conditioning (HVAC) systems and tend to be nearly incompressible (very low Mach number). The NETFLOW models and numerical methods used to predict these flows are documented in References [1] and [2].

This report will focus on the NETFLOW theoretical models used to analyze high Mach number fully compressible transonic flows in piping networks.

NETFLOW's high Mach number models are accessed through a keyword driven user interface that permits the user to predict the transport of multispecies compressible gas mixtures through arbitrary arrangements of vessels, tubes, valves and flow branches. The User's Manual for this keyword-driven interface is provided here in Appendix A. The User's manual is automatically updated each time new features are added to NETFLOW. The most current User's Manual is always available to the user as a text file named "netflow.txt" which is part of the NETFLOW code distribution package. The User's Manual in Appendix A is provided so that readers of this report can see how the various theoretical models are accessed when using NETFLOW.

NETFLOW's methodology for describing the transport of gases is derived from early attempts at modeling the flow of water-steam mixtures in nuclear reactor cooling systems. The methodology is described in detail in References [3] and [4]. Flows through cooling systems are inherently three-dimensional and transient. In order to make the problem more tractable, the methodology attempts to represent these flows using a system of one-dimensional (along the flow direction) transient ordinary differential equations. Flows along tubes are described with "zero-dimensional" transient conservation equations. By "zero-dimensional" we mean that the contents of a modelled vessel (or piping control volume) are assumed to be well-mixed and uniform in space at any point in time. The inherent multi-dimensional aspects of these flows are modelled using heat transfer and pressure drop correlations. For the most part these correlations are obtained from the literature. An example of such a correlation is the Moody friction factor correlation [5] which is used to describe pressure drop along a tube due to transverse velocity gradients near the pipe wall. In this case the correlation serves as a means of accounting for the multi-dimensional behavior of tube flow even though the modeling equation for fluid momentum only accounts for spatial changes in the flow direction. Correlations like these are usually developed for steady flow. Their use in NETFLOW assumes that even transient flows can be modeled as "quasi-steady" over most time domains. For the most part, this is true but there are time domains, usually very short, over which flows are not quasi-steady. An example of such a domain is the first few milliseconds after a valve, that is downstream of a pressure tank, is opened or closed. In this brief period of time shocks and rarefaction waves travel through the adjacent tubing reflecting back and forth multiple times before true quasi-steady flow is established. For these highly transient flow periods it would probably be more accurate to model the flow as inviscid (frictionless) rather than applying a quasi-steady friction correlation. In practice, however, only negligible errors are introduce when Moody friction is applied over the entire time since most transfers are quasi-steady.

The first dedicated computer code utilizing the previously described methodology was TOPAZ (Transient One-dimensional Pipe-flow AnalyZer). TOPAZ is described in detail in References [6-10]. The system of ordinary and algebraic equations which make up a TOPAZ model are solved using the differential-algebraic system solver developed by Petzold [11].

In many ways NETFLOW is nearly identical to TOPAZ in its modeling methodology. NETFLOW represents a second generation in modeling problems with more extensive models for flow boundary conditions and gas mixture thermodynamics, improved correlations, the ability to model containment heat conduction and a slightly different, but equivalent, spatial finite differencing method when modeling tubing runs.

In Section 2.0 the flow conservation equations and model topology utilized in NETFLOW modeling is discussed. NETFLOW thermodynamics and property evaluation is discussed in Section 3.0. Section 4.0 presents various constitutive models designed to account for multidimensional effects not directly modelled by NETFLOW. The solution of the NETFLOW conservation equations is discussed in Section 5.0. Section 6.0 presents the finite difference wall heat conduction model that is available to NETFLOW users. The end of the report contains a number of Appendices that support the main text of the report.

NETFLOW CONSERVATION EQUATIONS

The following five equation types are used to build a NETFLOW model for a system of interest:

1. Gas species mass conservation equations
2. Gas mixture energy conservation equations
3. Gas mixture momentum conservation equations
4. The equation of state
5. Wall containment heat conduction

In this section the conservations equations for species mass, mixture energy and mixture momentum will be discussed. Later sections will address the equation of state, containment heat conduction and the various correlations that are used to account for multidimensional behavior.

NETFLOW Spatial Discretization

Figure 1a shows a typical gas flow network composed of three vessels, three tubes and one flow branch linking the three tubes together. In order to model this network it is necessary to discretize the network into a number of control volumes called "nodes." One possible discretization is shown in Figure 1b. In this case each vessel and the flow branch are represented by a single "node" or control volume. These nodes are numbered 1 through 4 in the Figure. Each length of tubing is represented by a series of nodes. In this case one tube is made up of 23 nodes, another 15 nodes and the third 10 nodes. Hence for this model the network has been divided into a total of 52 nodes or control volumes. These nodes represent locations where mass of each gas species and the energy of the gas mixture must be conserved. Thus 52 gas mixture energy equations must be satisfied. The number of gas species mass conservation equations that must be satisfied is 52 times the number of species present in the gas mixture.

All nodes in the network model are linked to each other by flow "paths". These paths are not shown in Figure 1b but their positions align with the interfaces between the nodes. In this model there are 51 interfaces between the 52 nodes. Hence there are 51 locations or paths in the model where the gas mixture momentum must be satisfied. Note that the physical locations where momentum conservation equations are satisfied do not aligned with the locations where mass species and mixture energy are satisfied. It is simply not possible to co-locate these positions without causing a numerical instability called "pressure checker-boarding" as discussed in Reference [13].

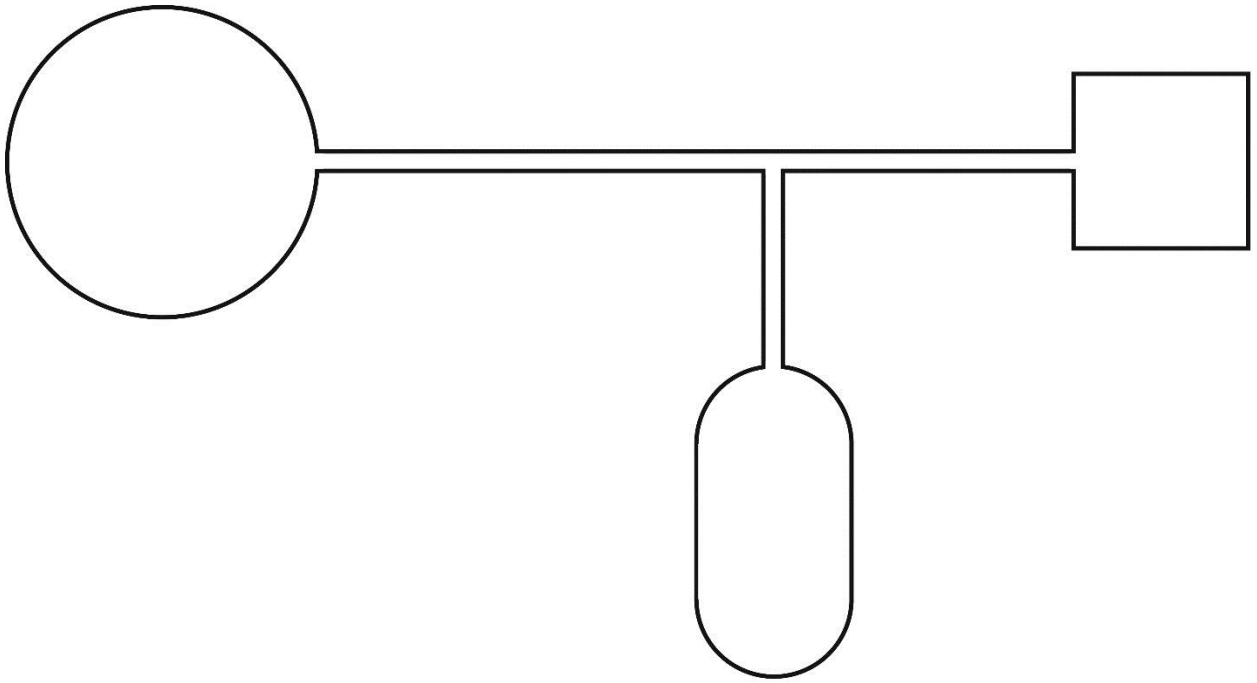

a) Tubing and pressure vessels

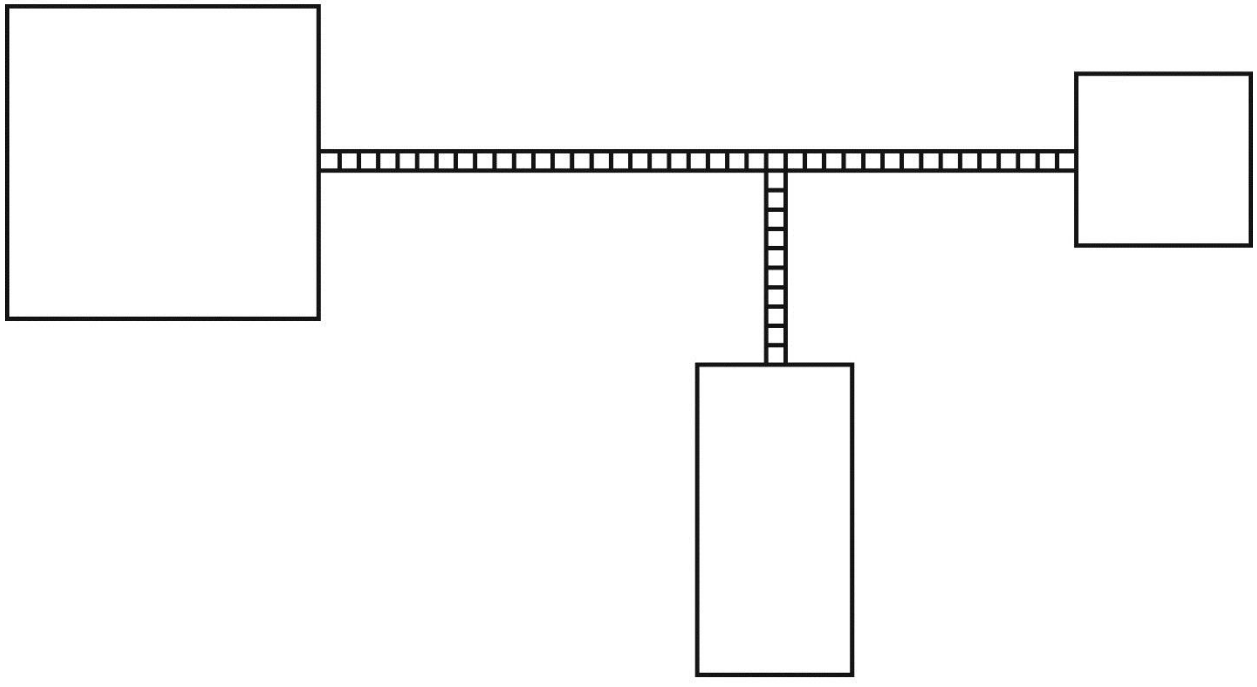

b) "Nodalization of tubing and pressure vessels

Figure 1. NETFLOW model representation.

It is useful to think of nodes as scalar control volumes where all system scalars are computed (*e.g.* the density of each gas species, the mixture internal energy, pressure, enthalpy, *etc.*). The paths represent control volumes (centered at the nodal interfaces) where the vector quantities such as mass flow rate or velocity are computed. These are vector quantities since they have both magnitude and direction. Their directions are limited to either forward flow (a positive flow from the upstream node to the downstream node) or reverse flow (a negative flow from the downstream node to the upstream node).

In some cases it is necessary to extrapolate properties from the place where they are computed using the appropriate conservation equation to other locations in the flow. For example the mass flow rate for gas in a node must be extrapolated from the mass flow rates computed at adjoining paths. This is usually accomplished using simple averaging techniques as will be discussed later. In a similar manor, some scalar properties for paths must be extrapolated from adjacent nodes. In this case they are almost always taken from the "upwind" or "upstream" node rather than from an averaging of the upstream and downstream nodal values. Upwinding is used because it tends to be more stable for subsonic flow. Furthermore, for a sonic or "choked" flow, a simple averaging of upwind and downwind scalars would not make since a choked flow has no communication with events or properties that are downstream of it.

The topology of nodes and paths is further demonstrated in Figure 2-4. Figure 2 shows a node connected to an arbitrary number of paths (a total of J_{MAX} paths). The volume of the node is shown as the shaded grey area and corresponds to the one half the volume of all connected paths plus an additional volume if the node is to represent a pressure vessel or a flow-branch node.

Figure 3 shows the simplest possible system consisting of two vessels connected by a single path. The upstream vessel and downstream vessels are labeled N_{UP} and N_{DN} respectively. The path connecting these two nodes has a cross-sectional area A_J and a Length L_J. The physical volume of the path is partitioned equally between the two nodes as indicated by the grey and blue shading. Hence the volume of node N_{UP} is equal to the volume of the upstream vessel plus one half of the connecting path. Similarly the volume of node N_{DN} is equal to the volume of the downstream vessel plus the other half of the connecting path.

Figure 4 shows part of a discretized tube or pipe that is made up of a string of alternating nodes and paths. In this case all the nodes and paths have identical flow areas and the volume of each node is equal to one half of the two paths attached to it, *i.e.* no additional volume is added since these nodes do not represent vessels.

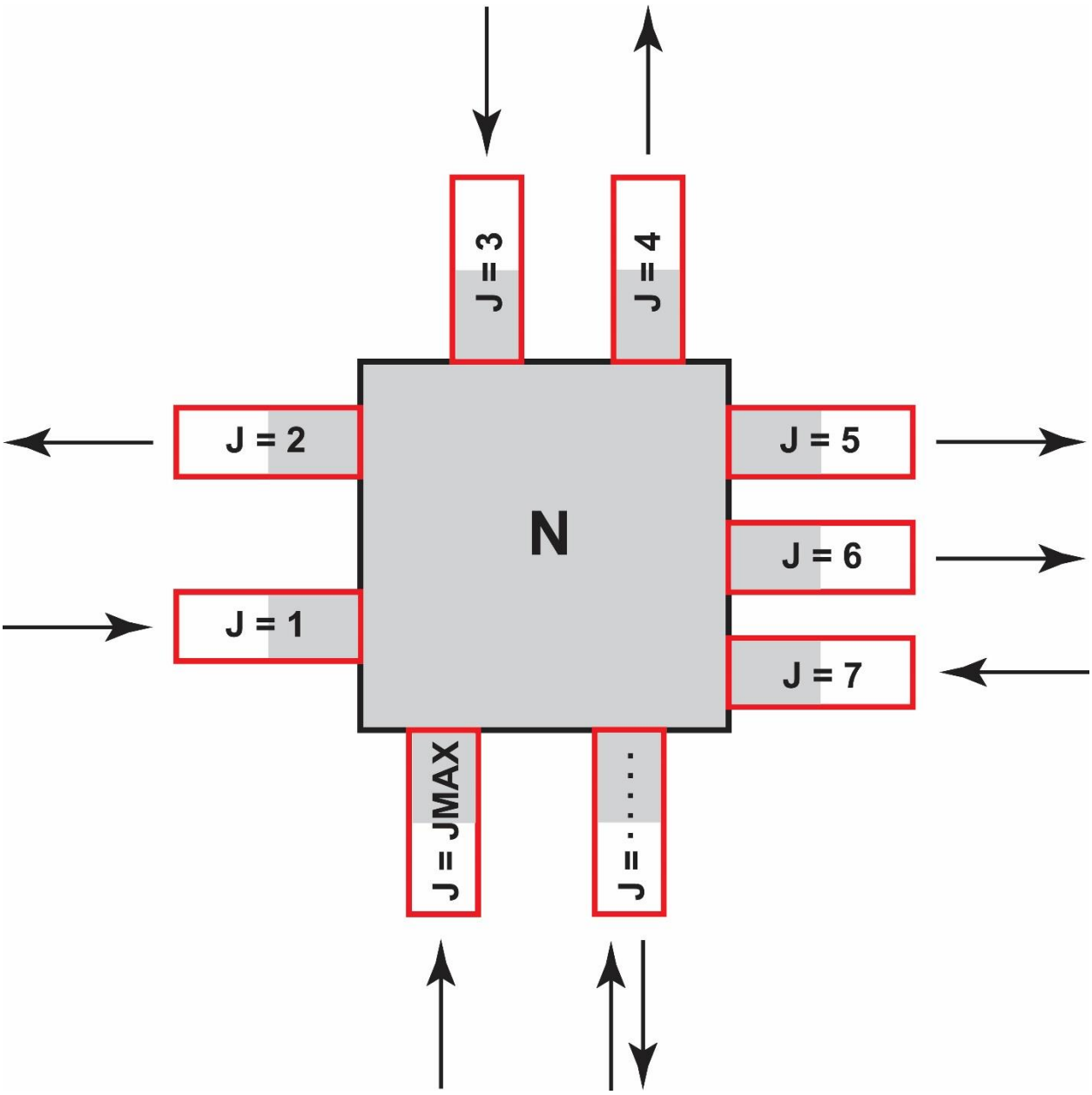

Figure 2. NETFLOW NODE connected to multiple flow PATHS.

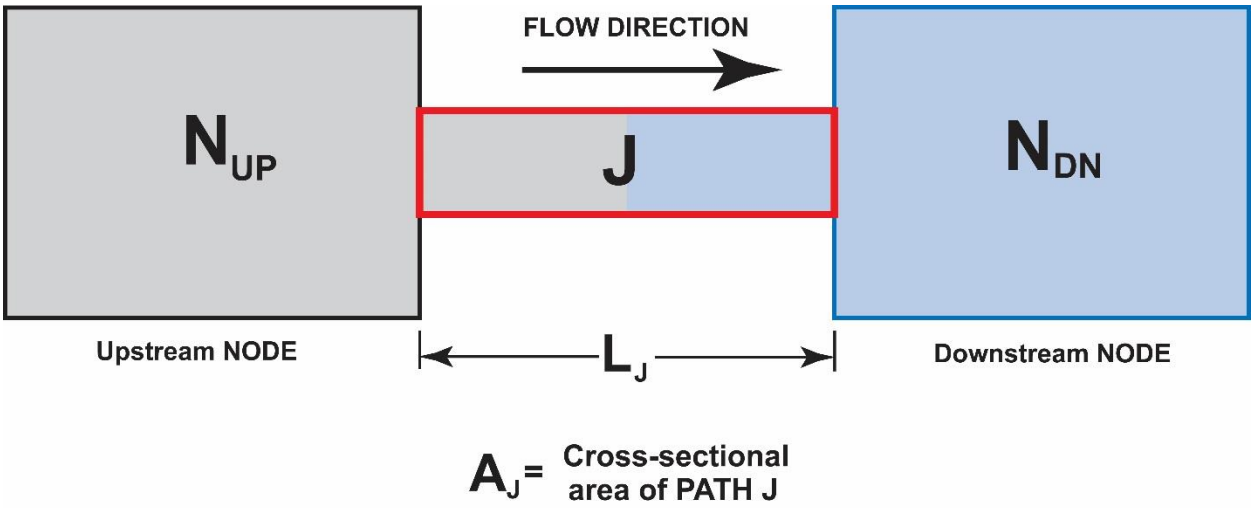

Figure 3. NETFLOW PATH transporting a gas mixture between two NETFLOW NODES.

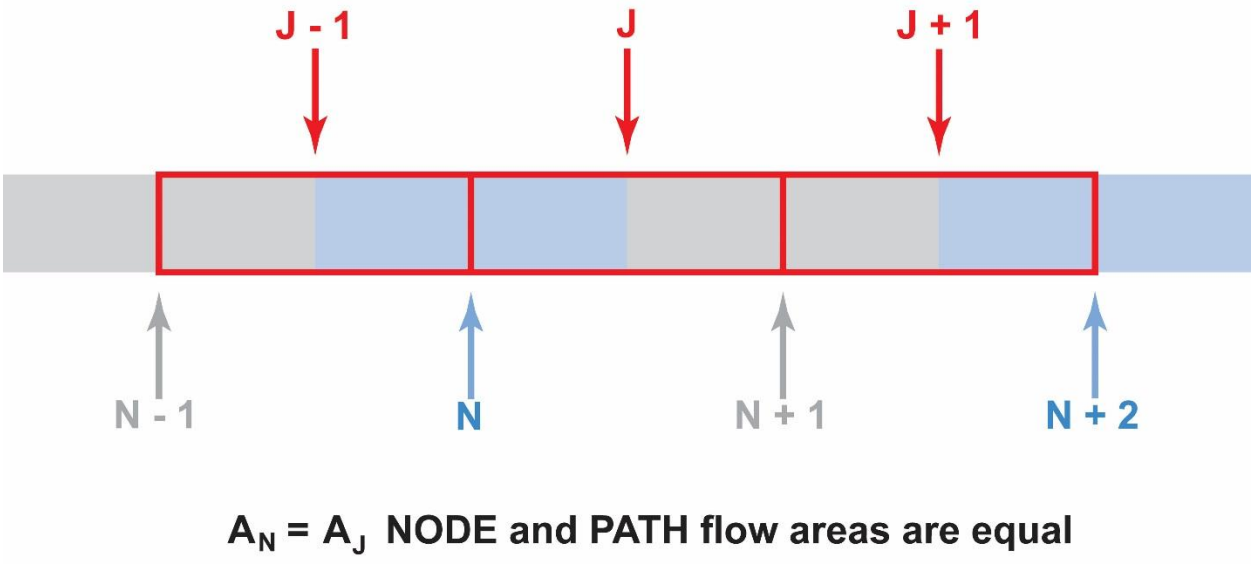

Figure 4. NEFLOW NODES and PATHS linked together to form a one-dimensional-transient finite difference representation for flow in a pipe.

Species Mass Conservation Equation

In general, NETFLOW treats the transport of compressible gas "mixtures", hence any modeling constraint that accounts for continuity must address each gas species that forms the mixture.

The set of species mass conservation equations for the node shown in Figure 2 is given by:

$$\frac{dM_{N,K}}{dt} = \sum_{J=1}^{J=J_{MAX}} S_J \, Y_{J,K} W_J + Y_{N,K} \dot{M}_N \tag{2.1}$$

where K, the species number that designates a particular species. K varies from 1 to K_{max}, the maximum number of species in the gas. The remaining notation is defined below:

$M_{N,K}$ = mass of species K in node N

$Y_{N,K}$ = mass fraction of species K in node N

$Y_{J,K}$ = mass fraction of species K in path J

S_J = sign of the flow at an attached path J

= +1 for flows entering node N

= -1 for flows exiting node N

W_J = mass flow rate through path J

$\dot{M}_N$ = mass generation rate in none N

Each species K conservation equation simply states that the time rate of change for any species mass K within a control volume is equal to the sum of incoming mass flow rates of K minus the outgoing mass flow rates of K plus the rate at which the K is generated within the control volume. The last term is generally zero although the user has the option to specify a generation (or depletion) rate for K.

$Y_{J,K}$ is identically equal to $Y_{NUP,K}$ where NUP refers to the node that is "upwind" of path J.

M_N, the total mass of the gas mixture at node N is computed using:

$$M_N = \sum_{K=1}^{K=K_{MAX}} M_{N,K}. \tag{2.2}$$

Mixture Energy Conservation Equation

The mixture energy conservation for the nodal control volume shown in Figure 2, is a simple statement of the First Law of Thermodynamics, namely, "the time rate of change of energy within the node is equal to sum of the incoming energy flow rates minus the outgoing energy

flow rates plus the heat transferred from the containment walls plus any internal energy generated (or removed) from the control volume:"

$$\frac{d}{dt}\left[M_N\left(u_N+\frac{v_N^2}{2}\right)\right]=\sum_{J=1}^{J=J_{MAX}} S_J\, W_J\left[u+\frac{P}{\rho}+\frac{v^2}{2}\right]_J+h\,A_s\,[T_w-T_n]+\dot{E}_N \quad (2.3)$$

where,

M_N = mass of gas mixture in node N

u_N = internal energy per unit mass for the gas mixture in node N

V_N = velocity of gas mixture in node N

S_J = sign of the flow at an attached path J

= +1 for flows entering node N

= -1 for flows exiting node N

W_J = mass flow rate through path J

$\left[u+\frac{P}{\rho}+\frac{v^2}{2}\right]_J$ = the sum of internal energy per unit mass plus the flow work per unit mass plus the kinetic energy per unit mass for the flow stream entering/exiting at the path J.

The quantity u, is the internal energy per unit mass. The flow work per unit mass is $\frac{P}{\rho}$ (pressure divided by density) and the kinetic energy per unit mass is $\frac{V^2}{2}$.

h = the Newton's Law heat transfer coefficient for heat transfer from the wall to the node N.

A_S = the surface area of the containment wall surrounding node N

T_W = the wall surface temperature

T_N = the gas mixture temperature in node N

$\dot{E}_N$ = the energy generation rate in node N

The energy equation neglects changes in potential energy. The heat transfer coefficient used in describing the heat exchange between the containment wall and the gas mixture in the node is determined from a number of models available to the user. These models are discussed later. The last term, $\dot{E}_N$, is generally zero although the user has the option to specify an energy generation (or depletion) for the gas in any node.

The quantities u, P, ρ and v in the path flow term $\left[u + \frac{P}{\rho} + \frac{v^2}{2}\right]_J$ are obtained from the node "upwind" of the path J. For flow exiting the node N these values would be u_N, P_N, ρ_N, and v_N. For flows entering node N these values would be from the node upstream of the incoming flow path or u_{NUP}, P_{NUP}, ρ_{NUP}, and v_{NUP}. (These nodes are not shown in Figure 2.)

The node mean velocity, v_n, is calculated from the following expression,

$$v_N = \frac{W_N}{A_N \rho_N} \tag{2.4}$$

where W_N is the nodal mass flow rate, $A_{N,}$ is the nodal cross-sectional flow area and ρ_N is the density of the gas mixture in the node.

The nodal mass flow rate must be interpolated from the incoming and outgoing path mass flow rates using

$$W_N = \frac{1}{2}\left(\sum_{IN} W_J - \sum_{OUT} W_J\right). \tag{2.5}$$

Equation (2.5) is a general expression for averaging multiple path flows into and out of a node, *i.e.* the situation shown in Figure 2. For a simpler topology, like that shown for the nodes in Figure 4, it is easily seen that the flow rate for a node is determined from the simple average of the incoming path flow rate and the outgoing path flow rate. For a node acting as a reservoir the nodal flow rate is equal to half of the outgoing path flow rate. Similarly for a node acting as a receiver, the nodal flow rate is equal to half of the incoming path flow rate. As previously mentioned all flow rates and velocities in NETFLOW paths are vector quantities having both magnitude and direction. Hence all path mass flow rates and velocities have a sign associated with them indicating the direction of flow. Nodal mass flow rates and velocities are always positive since there is no vector information stored at nodes.

Mixture Momentum Equation

Mixture momentum equations are calculated for each path in a NETFLOW simulation. Consider the path J shown in Figure 3 connecting an upstream node NUP to a downstream node NDN. The path has a length L_J and a constant cross-sectional flow area A_J. The momentum equation for path J is a straightforward application of Newton's second law which states that the time rate of change of momentum within the path volume is equal to the rate of momentum entering minus the rate of momentum leaving plus the sum of the forces applied to the path volume, *i.e.*,

$$L_J \frac{d}{dt}\left(W_J\right) = A_j\left(\rho_{NUP} v_{NUP}^2 - \rho_{NDN} v_{NDN}^2\right) + A_j\left(P_{NUP} - P_{NDN}\right) - \left(K_f + K_A + K_L\right)\frac{1}{2} W_j \left|V_j\right|, \tag{2.6}$$

where,

ρ_{NUP} = density of the gas mixture in the upstream node

V_{NUP} = velocity of the gas mixture in the upstream node

ρ_{NDN} = density of the gas mixture in the downstream node

V_{NDN} = velocity of the gas mixture in the downstream node

P_{NUP} = Pressure of the gas mixture in the upstream node

P_{NDN} = Pressure of the gas mixture in the downstream node

K_f = form loss coefficient due to wall frictional pressure drop

K_A = form loss coefficient due to expansion or contraction and the flow path boundaries

K_L = a user specified form loss

Note that centered differences are used to determine upstream and downstream pressures and momentum. The first term on the right hand side represents the change in momentum entering and leaving the path J. The second term is the sum of the pressure forces acting on path J. The last term is a loss term that represents frictional drag on the path side walls, losses associated with an area change at the boundary of the flow path and any additional loss specified by the user. Using the absolute value of the path velocity $|V_J|$ insures that the loss term always opposes the direction of flow.

The frictional form loss takes the form,

$$K_f = \frac{fL_J}{D_h} \tag{2.7}$$

where f is the Moody friction factor for pipe or duct flow and D_h is the hydraulic diameter of the flow path. The user can provide a constant (including 0) for f or as is discussed later, a mathematical relationship in which f is a function of the local Reynolds number.

The form loss K_A for is intended to account for losses due to expanding and contracting flow at the boundaries of the path. In Figure 3 there is a contraction in flow at the upstream end of the flow path and an expansion at the downstream end, References [14] and [15] provide form loss models based on incompressible quasi-steady flow across and area change. These models are built into NETFLOW and take the form,

$$K_A = \frac{1}{2}\left(1 - \frac{A_J}{A_{NUP}}\right) + \left(1 - \frac{A_J}{A_{NDN}}\right)^2 \; for \; W_J \geq 0 \tag{2.8}$$

$$K_A = \frac{1}{2}\left(1 - \frac{A_J}{A_{NDN}}\right) + \left(1 - \frac{A_J}{A_{NUP}}\right)^2 \quad for \;\; W_J < 0 \tag{2.9}$$

Equations (2.8) and (2.9) should be considered as approximations when dealing with highly compressible quasi-steady flows (i.e. Mach numbers greater than 0.3).

User specification of the form loss, K_L allows the user to specify a form loss based on experimental data, providing such data exists.

Choked Flow

In quasi-steady compressible flow, the flow at area expansions can become choked. The process of flow choking is discussed in many references including Shapiro [16]. A choked flow occurs when the pressure downstream of the choke point becomes so low that the flow speed at the choke point reaches the sonic velocity. Downstream of the choke point the flow becomes supersonic until a series of shock waves restores the flow to subsonic conditions. The one-dimensional mixture momentum Equation (2.6) cannot be used to describe choked flow since downstream pressure signals cannot propagate upstream to impact the flow rate. Saying it another way, the flow at the choke point has no knowledge of the pressure downstream and as result is unaffected by this pressure unless forces driving the flow cause the flow to decelerate. When the flow decelerates, the velocity at the choke point drops below it sonic value and Equation (6) can once again be used to describe the flow rate.

In order to understand how NETFLOW deals with choked flow, it is useful to rewrite Equation (6) in the following form,

$$L_J \;\; \frac{d}{dt}\left(W_J\right) = RHS \tag{2.10}$$

where "*RHS*" are the terms on the Right Hand Side of Equation (6). If we think of Equation (2.6) as an expression of Newton's Second Law as applied to a fluid (which it is), it is easy to see that when *RHS* is positive the flow is accelerating and when *RHS* is negative the flow is decelerating. We can use this knowledge to establish the rules for describing choked and unchoked flow in NETFLOW.

For unchoked flow where W_j is less than the sonic flow rate, $W_{J\,SONIC}$, Equation (2.6) is used to determine the path flow rate. Because of our upwinding of scalar properties at path locations, the sonic flow rate for a path is described by,

$$W_{J\,SONIC} = \rho_{NUP} A_j C_{NUP} \tag{2.11}$$

where C_{NUP} is the speed of sound in the gas mixture at the upstream node. The speed of sound is a thermodynamic property that is determined from the equation of state for the mixture.

When the flow is choked, Equation (2.11) is used to determine the path flow rate. Equation (2.11) will continue to be used to describe the path flow rate until RHS changes sign signaling a deceleration of flow below $W_{J\,SONIC}$. Hence we can summarize the NETFLOW choking and

unchoking rules for a potential choking path *(i.e.* a path where the flow expands or $A_{NDN} > A_J$) using the following statement:

"Equation (6) is used until $W_J = W_{J\,SONIC}$ then Equation (2.11) is used until *RHS* changes sign."

As discussed in the next section, the NETFLOW conservation equations are solved using the DASKR differential algebraic solver [12]. DASKR requires that all equations be continuous over time. Switching between Equations (6) and (2.11) clearly violates this requirement. This problem is overcome by employing the "root finding" capability in DASKR. Root finding is used to continuously monitor the choked and unchoked state of all paths. When a transition between choked and unchoked flow is detected, DASKR attempts to find the exact point in time when the transition occurs. It then stops the calculation and substitutes the appropriate path flow equation and restarts the problem with the appropriate initial conditions.

When the choking and unchoking rules are applied, it can be shown that NETFLOW and the root finding capability of DASKR properly chokes and unchokes the flow at appropriate upstream/downstream pressure ratios. The actual region of supersonic flow and shock structure downstream of the choke are not being modeled in NETFLOW but the proper flow rates for unchoked and choked flow are preserved.

Alternate Path Flow Equations

Equations (2.6) and (2.11) represent the most often used relationships for describing NETFLOW path flows for high Mach number flows. They are used to describe flow transitions from vessels to tubing, flow through tubing with and without area changes and flow transitions from tubing to vessels. The accuracy of these equations is heavily dependent on our ability to characterize the form loss coefficients K_f, K_A, K_l. These form losses are intended to account for all wall frictional effects and multidimensional flow effects not directly modeled by the one-dimensional flow momentum equation. Often these form losses are unknown or are not adequately represented by the NETFLOW "built-in" form models. We know, for example, that the area change form loss expressions defined by Equations (2.8) and (2.9) are intended for incompressible flow in which the local Mach number is less than approximately 0.3. What if the local Mach number is 0.9? Similarly, we know that the characterizing the frictional pressure loss K_f using the Moody friction factor is adequate for quasi-steady fully developed flow in a straight tube but what if the flow is not fully developed or the tube is not straight? (It often takes more than 50 tube diameters of flow at the entrance of the tube before the flow is fully developed.) In these cases, the "build in" NETFLOW form loss models must be regarded as approximations.

In addition to Equations (2.6) and (2.11), there are several additional quasi-steady relationships available for describing path flows that may be more appropriate for describing path flows. These include models for isentropic, porous media, and valve flows.

Isentropic Flow

In some cases the previously described flow equations may be less accurate than just assuming isentropic flow through the path. This is sometimes true for the case where flow is being accelerated from stagnation conditions in a reservoir to high speed flow in the exit tubing. The

previously described finite differencing and the area change loss relationships given in Equations (2.8) and (2.9) may be less accurate than assuming isentropic flow. See Appendix B for a more detailed discussion.

The NETFLOW isentropic model for an expanding flow is identical to the model outlined by Bird, Stewart and Lightfoot [17] for flow of an ideal gas. For flow from an upstream node N_{UP} to a downstream node N_{DN} through path *J*, we first determine the path flow Mach Number using scalar properties from the upwind node:

$$Ma_J = v_{NUP}/\sqrt{\gamma_{NUP} RT_{NUP}} \tag{2.12}$$

where γ is the ratio of specific heats (C_p/C_v).

The upstream total pressure, $P_{o_{NUP}}$ and total density, $\rho_{o_{NUP}}$ is computed from the upstream static pressure, P_{NUP} and upstream static density ρ_{NUP} in the usual way (see *e.g.* [16]),

$$P_{o_{NUP}} = P_{NUP}\left[1 - .5(\gamma - 1)Ma_J{}^2\right]^{\gamma/(\gamma-1)} \tag{2.13}$$

$$\rho_{o_{NUP}} = \rho_{NUP}\left[1 - .5(\gamma - 1)Ma_J{}^2\right]^{1/(\gamma-1)} \tag{2.14}$$

We define the pressure ratio for the path to be

$$P_r = P_{NDN}/P_{o_{NUP}}. \tag{2.15}$$

It can be shown (see *e.g.* [17]) that the critical pressure ratio, Pr_{CRIT}, at which choking occurs is given by

$$Pr_{CRIT} = 2/(\gamma + 1)^{\gamma/(\gamma-1)} \tag{2.16}$$

The isentropic path flow model may now be summarized as:

$$W_J = A_j\sqrt{\frac{2P_{o_{NUP}}\rho_{o_{NUP}}\left[Pr^{2/\gamma} - Pr^{(\gamma-1)/\delta}\right]}{\gamma-1}} \quad \text{for Pr} > Pr_{CRIT} \tag{2.17}$$

$$W_J = A_j\sqrt{\frac{2P_{o_{NUP}}\rho_{o_{NUP}}\left[Pr_{CRIT}^{2/\gamma} - Pr_{CRIT}^{(\gamma-1)/\gamma}\right]}{\gamma-1}} \quad \text{for Pr} \leq Pr_{CRIT} \tag{2.18}$$

where Equation (2.17) applies to unchoked flow and Equation (2.18) applies to choked flow. At this writing the complete choking/unchoking behavior of the isentropic path model is not fully implemented. The root finding capability of DASKR is not used to choke and unchoked the flow at an isentropic path. It is therefore recommended that the isentropic path be only applied to contracting flows (*e.g.* the transition between an evacuating reservoir and the exit tubing) since a

transition to choked flow can never occur in a contracting flow [16]. If the isentropic path is used at a location of expanding flow, numerical instabilities are likely to result.

Porous Media Flow

NETFLOW allows the user to specify a porous media flow for a path. The previously described path flow models are then replaced by the Shugard – Van Blarigan porous media model documented in Reference [18]. The implementation and Validation of this model in NETFLOW is fully documented in Reference [19] and will not be presented.

Valve Flow

For those cases when a flow path is used to simulate a valve that has been experimentally characterized using flow rate and pressure drop data, the valve flow model developed by B. L, Bon, 8254 [20] may be used. The model accounts for both choked and unchoked flow through the valve. Three experimentally obtained constants, α_1, α_2 and α_3 must be supplied by the user. Flow through the valve is dependent on two pressure drop parameters β and β_{CRIT} which are defined as follows:

$$\beta = 1 - P_{NDN}/P_{NDN} \tag{2.19}$$

$$\beta_{CRIT} = \frac{-\alpha_1 + \sqrt{\alpha_1^2 + 4\alpha_2\alpha_3}}{2\alpha_2}. \tag{2.20}$$

The valve path model may be summarized as

$$W_j = \frac{\sqrt{\beta(\alpha_1 + \alpha_2\beta)}}{\delta} \quad \text{for } \beta < \beta_{CRIT} \quad \text{(unchoked flow)} \tag{2.21}$$

$$W_J = \frac{\sqrt{\alpha_3}}{\delta} \quad \text{for } \beta \geq \beta_{CRIT} \quad \text{(choked flow)} \tag{2.22}$$

where the parameter δ is given by

$$\delta = \frac{\sqrt{RT_{o_{NUP}}}}{P_{o_{NUP}} A_J}. \tag{2.23}$$

In Equation (2.23) $P_{o_{NUP}}$ is the upstream stagnation pressure as defined by Equation (2.13) and $T_{o_{NUP}}$ is the upstream stagnation temperature defined by

$$T_{o_{NUP}} = T_{NUP}[1 + 0.5(\gamma - 1)Ma_{NUP}^2]. \tag{2.24}$$

The choking/unchoking behavior of the valve flow model is fully implemented into NETFLOW, *i.e.*, the rooting finding capabilities of DASKR are utilized in order to properly transition between Equations (2.21) and (2.22).

Open and Closing Flow Paths

In some cases it may be desirable to open and close flow paths during a simulation. Opening and closing flow paths is supported for the unchoked and choked tube flow momentum Equations (2.6) and (2.11), the unchoked isentropic flow path, Equation (2.17) and the unchoked and choked experimentally characterized valve flow model, Equations (2.21) and (2.22). Opening and closing of these flow paths is accomplish by multiplying the right hand side of the appropriate equation by a scaling factor F

$$F = A(t)/A_J \tag{2.25}$$

where A_J is the fully open cross-sectional path flow area and $A(t)$ is the time varying flow area which varies between 0 and A_J. The user specifies a time duration over which the valve opens or closes. During this opening and closing time the factor F varies between 0 and 1 in a linear fashion to scale the path flow. It is important to make flow path opening times as short as possible since actual flow during the opening and closing periods is only approximate.

The process described above makes it possible to open and close flow paths using the mixture momentum equation alone, *i.e.*, it is not necessary to rely on the root finding capability in DASKR to transition between open and closed paths.

NETFLOW THERMODYNAMICS AND PROPERTY DETERMINATION

The flow conservation equations described in the previous section are used to determine the mass of each species at all nodes, $M_{N,K}$ the internal energy of the mixture at all nodes, U_N and the flow rate of the mixture at all paths, W_J. The remaining properties in the flow are determined from extrapolation and from thermodynamics. Examples of extrapolated properties include the mass flow rates at all nodes and the scalar properties at paths. As mention previously nodal mass flow rates are extrapolated from the computed flow rates at all paths using Equation (2.5) and all the scalar properties at paths are extrapolated from upwind nodal values.

The following are some additional properties that are computed from the above mentioned variables and the flow geometry:

Mixture Nodal Density – The mixture density, ρ_N, at a node is determined from the nodal mixture mass, M_N (Equation 2.2), and the volume of the node, V_N, using

$$\rho_N = \frac{M_N}{V_N}. \tag{3.1}$$

Mixture Nodal Velocity – The mixture nodal velocity, v_N, is determined from the mixture nodal density, ρ_N, the nodal cross-sectional flow area, A_N, and the nodal flow rate, W_N using

$$v_N = \frac{W_N}{A_n \rho_N}. \tag{3.2}$$

Mixture Path Velocity – The mixture path velocity, v_J, is determined from the mixture path density (extrapolated from the upwind node), ρ_{NUP}, the path cross-sectional flow area, A_J, and the path flow rate, W_J, using

$$v_j = \frac{W_j}{A_j \rho_{NUP}}. \tag{3.3}$$

Species Nodal Mass Fractions – The mass fraction of species *K* at node *N*, denoted by the symbol $Y_{N,K}$, is determined from the species nodal mass, $M_{N,K}$ (Equation 2.1) and the total nodal mass, M_N, (Equation 2.2) using

$$Y_{N,K} = \frac{M_{N,K}}{M_n}. \tag{3.4}$$

Mixture Nodal Molecular Weight – The molecular weight of a mixture at node N, denoted with the symbol MW_N, is determined from the species molecular weights, $MW_{N,K}$, and the species mass fractions using:

$$MW_N = \frac{1}{\sum_{K=1}^{K-K_{MAX}} Y_{K,N}\, MW_{K,N}} . \quad (3.5)$$

The remaining properties that need to be determined are nodal properties that depend solely on the thermodynamics. In the discussion which follows we will present a set of assumptions and equations for the NETFLOW thermodynamic model. Since all properties being calculated are nodal properties, the subscript N will be dropped from the equations.

Although the DALTON model for a mixture of ideal gases can be used, the principle NETFLOW thermodynamic model is the Abel-Noble model developed by Chenoweth [21]. The equation of state is based on a simplified form of the van der Waals Equation of State (see e.g. Reference [22]). This equation of state is a real-gas equation of state that has a single constant and takes the following form:

$$P = Z\frac{\rho \bar{R}\, \mathrm{T}}{\mathrm{MW}} \quad (3.6)$$

where,

P = absolute pressure of the gas mixture

Z = Abel-Noble compressibility factor

ρ = mass density of the gas mixture

$\bar{R}$ = the universal gas constant

T = the temperature of the gas mixture

MW = the molecular weight of the gas mixture

b = the Able-Noble co-volume constant.

The Abel-Noble compressibility factor is given by,

$$Z = \frac{1}{1-b\rho} \quad (3.7)$$

Each species in the gas mixture has a unique co-volume constant b that permits the equation of state to be applied to pressures exceeding those commonly described by the ideal gas equation of state. The Able-Noble equation reduces to the ideal gas equation of state when $b=0$.

The rule for combining the b values for individual species to form a gas mixture b is a complex numerical procedure that is outlined here in Appendix C. The mixture b depends on the number of species, the values of b for each species and the mole fraction of each species in the mixture.

Assumptions used in the NETFLOW Able-Noble model are summarized as follows:

1. Constant specific heats are assumed.

2. Constant transport properties (thermal conductivity and fluid viscosity) are assumed.
3. Constant specific heats and transport properties are computed at ambient conditions.

The relationship between the mixture temperature, T, the mixture internal energy per unit mass, u and the mixture specific heat at constant volume, C_v follows from Maxwell's relations [18] and takes the from

$$C_v = \left(\frac{\partial u}{\partial T}\right)_v . \tag{3.8}$$

In light of the assumption constant specific heats and the assignment of $T=0$ when $u = 0$, it follows that

$$T = \frac{u}{C_v} \tag{3.9}$$

The mixture C_V is obtained from the species mass fractions, Y_k, and C_{vK} , the molar species specific heats at constant volume,

$$C_v = \sum_{K=1}^{K=KMAX} Y_K \, C_{vK} . \tag{3.10}$$

Similarly, mixture C_p is obtained from the species mass fractions, Y_k, and C_{pK} , the molar species specific heats at constant volume,

$$C_p = \sum_{K=1}^{K=KMAX} Y_K \, C_{pK} . \tag{3.11}$$

The thermodynamic definition of sound speed, C_s takes the form,

$$C_s{}^2 = \left(\frac{\partial P}{\partial \rho}\right)_s . \tag{3.12}$$

where s is the entropy per unit mass.

Using the Abel-Noble equation of state Equation (3.6) and Equation (3.12) together with Maxwell's relations, it can be shown that the sound speed of an Abel-Noble gas is given by

$$C_s = Z\sqrt{\gamma RT} \tag{3.13}$$

where the specific heat ratio, γ is ,

$$\gamma = \frac{C_v}{C_p} \tag{3.14}$$

and the mixture gas constant, R is given by,

$$R = \frac{\bar{R}}{MW}\,. \tag{3.15}$$

The thermodynamic definition for volume expansivity. β takes the form

$$\beta = \frac{1}{v}\left(\frac{\partial v}{\partial T}\right)_v \tag{3.16}$$

where v is the specific volume per unit mass.

Using the Abel-Noble equation of state Equation (2.6) and Equation (3.16) together with Maxwell's relations, it can be shown that the volume expansivity of an Abel-Noble gas is given by

$$\beta = \frac{1}{ZT}\,. \tag{3.17}$$

This completes the description of Abel-Noble thermodynamics used in NETFLOW modeling.

NETFLOW CONSTITUTIVE MODELS

NETFLOW utilizes a number of constitutive models that are intended to account for multidimensional effects not directly modeled by one and zero dimensional flow conservation equations. These constitutive models fall into two groups: Flow Models and Heat Transfer models.

Flow Models

These constitutive models account for multidimensional flow effects and wall friction effects. They are incorporated into the path mixture momentum Equation (2.6) as the form losses K_A, K_f and K_L. The "built in" form losses for low Mach number flow expansions and contraction have already been presented in the form of Equations (2.8) and (2.9). In order to account for the frictional form loss K_f it is necessary to provide a model for the friction factor f in Equation (2.7). The user may provide a constant friction factor or the "built in" friction factor model in which the friction factor varies as a function of the local Reynolds number and tube wall roughness. For laminar flow (very low Reynolds number) the friction factor takes the well-known (see e.g. [23]) form

$$f = 64/Re \tag{4.1}$$

where the Reynolds number is a dimensionless number specified by the local fluid velocity, v, fluid dynamic viscosity, μ, fluid density, ρ and the hydraulic diameter, D_h, *i.e.*,

$$Re = \frac{\rho v D_h}{\mu}. \tag{4.2}$$

The basis for the turbulent friction factor correlation in NETFLOW is the empirical data of Moody [5] which was mathematically represented by Colebrook and White [24] using the following implicit expression:

$$\frac{1}{f} = 1.74 - 2.0\ log\left(\frac{\epsilon/D_h}{3.7} + \frac{2.51}{Re\sqrt{f}}\right) \tag{4.3}$$

where ϵ is the interior tube wall roughness.

The actual procedure for calculation f in NETFLOW is identical to the method suggested by Churchill [24]. Churchill obtained a set of explicit algebraic equations for f which not only eliminated the need to solve the implicit Equation (4.3), but also provided for a numerically smooth transition between the laminar f in Equation (4.1) and the turbulent f in Equation (4.3).

It should be remembered that the "built in" model for the friction factor all assume that the flow in the tube is fully developed. This is important to remember since highly turbulent flow in a tube may require a significant length for the flow to become fully developed. Typical lengths often exceed fifty times the hydraulic diameter, D_h. During flow development the pressure drop could be larger than that computed by the built in friction factor model.

Heat Transfer

The NETFLOW interface provides the means to specify a constant heat transfer coefficient, *h* for calculating heat transfer between the gas mixture in a node and the interior wall of the node. The user can invoke isothermal conditions by specifying a very large *(e.g.*$1\ X\ 10^{20}$*)* heat transfer coefficient for a node. This will cause the contents of the node to take on the wall temperature. Equation (2.3) shows how this heat transfer coefficient is used in the mixture energy equation for the node.

Users may wish to take advantage of the NETFLOW "built in" variable heat transfer correlations in which *h* is dependent on local flow conditions in the node.

For forced convection heat transfer in a tube, NETFLOW computes both the laminar and turbulent Nusselt numbers (Nu_L and Nu_T respectively) and uses the largest of the two to compute the heat transfer coffiecient, i.e.,

$$h = k\,Nu_L/D_h \quad \text{for} \quad Nu_L \geq Nu_T \tag{4.4}$$

$$h = k\,Nu_T/D_h \quad \text{for} \quad Nu_T > Nu_L \tag{4.4}$$

where k is the gas mixture thermal conductivity and D_h is the tube or flow path hydraulic diameter.

The laminar Nusselt number from boundary layer theory is

$$Nu_L = 4.364. \tag{4.5}$$

The turbulent Nusselt number is based on the correlation developed by Dittus and Boelter [26]

$$Nu_T = = 0.23Re^{.8}Pr^{.4} \tag{4.6}$$

where *Re* is the Reynolds number is defined by Equation (4.2) and P_r is the mixture Prandtl number, a fluid property defined by

$$\Pr = \frac{C_p \mu}{k}. \tag{4.7}$$

The user invokes the tube flow forced convection heat transfer correlation when defining properties for a NETFLOW path. The heat transfer is applied to the path surface areas of the attached upstream and downstream nodes. The actual heat transfer is applied to the upstream and downstream node through the heat transfer term in Equation (2.3). As was the case for friction factors, tube flow forced convection heat transfer models apply to fully developed flow and must only be regarded as approximations for developing flow regions.

A number of built in heat transfer correlations are available for specifying heat transfer at node representing vessels or chambers. These models have been fully documented in References [27] and [28]. Only the final functional form of these correlations will be presented here.

When specifying heat transfer for a vessel, the NETFLOW user has the following options:

1. Isothermal vessel (user specifies a constant large h *(e.g.* $h = 1\,X\,10^{20}$)
2. Adiabatic vessel (user specifies a constant $h=0$)
3. Meyer free convection
4. Combined free and forced convection

The Meyer free convection correlation is based on a modified form of the Meyer correlation given in Reference [29]. The correlation is most appropriate for vessels acting as a gas reservoir that undergo a monotonic pressure decay as they empty. In this case the Nusselt number is determined from the maximum of the laminar and turbulent Nusselt numbers, *i.e.*,

$$Nu = \max(Nu_L, Nu_T) \tag{4.8}$$

where

$$Nu_L = .8331 Ra^{1/4} \tag{4.9}$$

$$Nu_T = .168 Ra^{1/3}. \tag{4.10}$$

The parameter R_a in Equations (4.9) and (4.10) is the Rayleigh number which is the product of the Grashof number, G_r and the Prandtl number, P_r and takes the form

$$Ra = Gr\,\mathrm{Pr} = \frac{g\beta(T-T_w)\rho^2 D^3}{\mu^2}\,\frac{C_p\mu}{k} \tag{4.11}$$

where g is the gravitational constant, β is the volume expansivity, D is the diameter of the spherical vessel or some other meaningful characteristic vessel dimension, and T-T_w is the temperature difference between the gas mixture in the vessel and the vessel wall temperature.

The combined free and forced convection vessel heat transfer model is suggested for nodes that act as receiver vessels. The combined model computes a forced convection Nusselt number based on the Reynolds number of the any incoming flow stream. If there are more than one incoming flow streams, Nusselt numbers for all the streams are calculated and the largest one is used to compute forced convection Nusselt number The forced convection Nussselt number for an incoming flow is computed from an equation first suggested by Means and Ulrich [30]:

$$Nu_{forced} = 6.694\left[Re\,\mathrm{Pr}\left(\frac{d}{D}\right)^2\right]^{-.632} \tag{4.12}$$

where the Reynolds and Prandtl number are computed from the incoming flow, d is the incoming flow diameter and D is the characteristic dimension of the vessel. The forced convection Nusselt

number attempts to account for the heat transfer effect of the incoming jet flow (usually supersonic) which may penetrate far into a filling vessel and contact the opposite wall. The combined model calculates a free convection Nusselt number using Equation (4.11) and a forced convection Nusselt number using Equation (4.12) uses the largest of the two as the combined vessel Nusselt number.

Once the Nusselt number is computed for a node acting as a vessel, the heat transfer coefficient for the vessel is computed in the usual way, *i.e.*,

$$h = k\frac{Nu}{D}. \tag{4.13}$$

The numerical coefficients and exponents appearing in the free convection vessel heat transfer coefficients (Equations 4.9-4.10) were determined from the experiments discussed in References [27] and [28]. In these experiments all reservoirs where oriented so that flows exited from the bottom and all receivers were oriented so the incoming flows entered at the top. Subsequent experiments have shown that heat transfer predictions are less accurate for other orientations. When proper orientations are used, the Meyer and the combined correlations for vessel heat transfer do an excellent job of predicting heat transfer in reservoirs. Heat transfer in a receiver, however, is much more complicated. The influence of one or more incoming jets together with large natural convection effects latter in the filling process make it difficult to characterize the heat transfer using the simple correlations presented here. For receivers, the user should expect that the combined model is only an approximation. References [27] and [28] demonstrate the accuracy one can expect under the best of circumstances.

The user may develop a unique vessel heat transfer correlation for a NETFLOW simulation by supplying a subroutine "user_h.f90." and the recompiling the code. In order to accomplish this, the user must have some knowledge of NETFLOW data encapsulation in order to access time varying properties at appropriate certain nodes and paths.

NETFLOW SOLUTION OF THE FLOW EQUATIONS

The set of differential-algebraic equations that make up the nodal species conservation equations, the nodal mixture momentum equations and the path mixture mass flow equations are solved using DASKR [12]. The numerically procedure is nearly identical to that used by DASSLRT [11], the differential-algebraic solver used by NETFLOW's predecessor TOPAZ [9]. The TOPAZ procedure is described in some detail on pages 38 and 39 of Reference [9] and will not be repeated here. The overall NETFLOW/ DASKR code architecture is identical to that of TOPAZ/DASSLRT which is illustrated in the flow chart of Figure 6 in Reference [9].

NETFLOW maps the conservation equations that make up the NETFLOW model into a single vector of equations, F_i, where i is the index for equation number. DASKR then operates on this vector using a predictor-corrector solution scheme with Newton iterations. If we assume that the total number of nodal species continuity, nodal mixture energy, and path mass flow equations is $imax$, then the vector F has $imax$ members. The flow conservations equations are mapped into the F vector in "residual" form with the nodal species mass equations first, the mixture momentum equations second and the path mass flow equations last. By residual, we mean that all terms in the conservation equations are moved to one side of the "equals" such that,

$$F_i[t, y_i(t), y_i'(t)] = 0,\ i = 1.2 \ldots., imax \tag{5.1}$$

where t is the independent variable time, $y_i,(t)$ is the vector of dependent variables, and $y_i'(t)$ is the first time derivative of $y_i(t)$. Members of the vector of dependent variables take on different form depending on which conservation equations is being represented by F_i. For the nodal species mass conservation Equation (2.1),

$$y_i = M_{N,K}\ . \tag{5.2}$$

For the nodal mixture energy Equation (2.3),

$$y_i = M_N(u_N + v_N^2/2). \tag{5.3}$$

For the path mixture momentum Equation (2.6),

$$y_i = L_j W_j. \tag{5.4}$$

For the path mixture momentum through an isentropic path, valve, or porous media flow,

$$y_i = W_J. \tag{5.5}$$

In order to understand the mapping between DASKR dependent variables $(y_i, i = 1, imax)$ and NETFLOW dependent variables $(M_{N,K}, L_j W_j,$ and $E_n = M_N(u_N + v_N^2/2)$), it is useful to think of a NETFLOW model having NMAX nodes, JMAX paths and KMAX species. For such a model the DASKR solution vector would have the following mapping:

$$Y_I = \begin{bmatrix} M_{1\,1} \\ M_{2\,1} \\ \cdot \\ M_{N\,1} \\ \cdot \\ M_{NMAX\,1} \\ M_{1\,2} \\ M_{2\,2} \\ \cdot \\ M_{N\,2} \\ \cdot \\ M_{NMAX\,2} \\ \cdot \\ M_{N\,K} \\ \cdot \\ M_{NMAX\,KMAX} \\ WL_1 \\ WL_2 \\ \cdot \\ WL_J \\ \cdot \\ WL_{JMAX} \\ E_1 \\ E_2 \\ \cdot \\ E_N \\ \cdot \\ E_{NMAX} \end{bmatrix} \qquad I = 1,2,\ldots,IMAX \tag{5.6}$$

During the solution of the equations the dependent variables are used to update all equations not directly solved by DASKR, *i.e.*, those quantities than can be directly computed from the dependent variables. These quantities are computed from Equations 2.5, 2.12 - 2.15, 2.19, 2.23 - 2.24, 3.1 – 3.7, 3.9 – 3,14, 3.16 – 3.14 and 4.1 – 4.13 prior to packing the residual vector F_i and on all returns from the DASKR solver.

DASKR takes control of the solution procedure returning to NETFLOW only to re-evaluate F_i, update properties, print intermediate results, restart calculations during root finding or when $t = t_{max}$, *i.e.*, when time has advanced to a maximum solution time determined by the user.

NETFLOW WALL HEAT CONDUCTION MODEL

Heat transfer to and from the flowing gas in a network is accounted for in the second to last term in the mixture momentum Equation (2.3), *i.e.*,

$$h\,A_s(T_w - T_N) \tag{6.1}$$

where T_N is the temperature of the gas in a node, T_w is the wall surface temperature adjacent to the gas, A_s is the surface area of the wall in contact with the node and h is the heat transfer coefficient. For most problems the wall temperature is assumed to be constant. However, NETFLOW provides the user with the option of accounting for a time varying interior wall temperature due to heat conduction through the containment wall. When this option is selected, NETFLOW models heat conduction through to wall using a one-dimensional transient heat conduction equation. Solution of the equation is accomplished using an explicit finite difference scheme. The features of wall heat conduction model are summarized as follows:

1. Heat conduction is assumed to be one-dimensional in space with heat flow taking place along a line normal to the interior wall.
2. Heat conduction is assumed to be transient in time. The temperature distribution in the wall is updated at fixed frequency. It proves convenient to make this frequency the same frequency at which results are printed to the NETFLOW output files. Hence, for example, if the user specifies that results be printed every .01 seconds, a new wall temperature distribution will be computed every .01 seconds. If the user chooses to use the wall heat conduction model, it is important to specify print intervals that are small enough to accurately capture the time evolving wall temperature distribution.
3. Each time the wall temperature distribution is updated, a series explicit time steps are taken to advance the heat conduction solution. The time step used is the largest stable explicit time step, a quantity automatically determined by NETFLOW. This time step is dependent on the spatial finite difference grid spacing through the wall and the thermal diffusivity of the wall. The initial temperature distribution in the wall during an update is taken to be the temperature distribution in the wall at a point in time when the previous print out was made. For the special case of time zero, the temperature distribution in the wall is assumed uniform and equal to the initial interior wall temperature. Assume, for example, that print frequency specified by the user is .01 seconds and NETFLOW has determined that the largest stable finite difference time step is .0001 seconds. Further assume that the current time of the NETFLOW simulation is 1.0 seconds and it is time to update the temperature distribution in the wall and print results. NETFLOW will then take the wall temperature distribution computed at 0.99 seconds and apply 100 explicit time steps to update the distribution to 1.0 seconds. Updating of the wall temperature will cause the interior wall temperature to change. This new interior wall temperature (T_w in Equation 6.1) will be used in all NETFLOW calculations for the node until time equals 1.01 seconds and it is time to update the wall temperature distribution and print results.

4. The surface area A_s over which heat conduction takes place will vary through the thickness of the wall depending on whether the wall geometry is planar, cylindrical (like a tube) or spherical (like a spherical pressure vessel).
5. The density, heat capacity and thermal conductivity of the wall material are assumed to be constant.
6. The user may specify that a wall be made up of multiple layers, each with its own density, heat capacity, thermal conductivity and spatial grid spacing.
7. Heat transfer from the outer surface of the wall to the ambient is assumed to result from Newton's law of cooling, (*i.e.* like Equation 6.1) with the heat transfer coefficient, h_{amb} and ambient temperature, T_{amb} constant. h_{amb} and T_{amb} are specified by the user.

The heat conduction model described above is somewhat decoupled from the NETFLOW transport model. The time varying value of the interior wall temperature provides the link between the two models. Since this temperature is only updated at the output print frequency, the coupling between the two models tends to be "loose" compared to the coupling that would be achieved by making all the interior wall temperatures part of the solution vector in Equation (5.1). Unfortunately, including all the finite difference wall temperature in Equation (5.1) would greatly increase computational times and could lead to increased difficulties in achieving a solution. Numerical studies have shown that the loose coupling described above makes it possible to add a wall heat conduction calculation to a NETFLOW simulation with a negligible increase in computational time. Any inaccuracies associated with the loose coupling can be easily discovered by exercising the NETFLOW model with several different printing frequencies.

The NETFLOW wall heat conduction model will be explained for a wall made up of a single layer. Extension to walls having multiple layers is straightforward.

The one-dimensional transient heat conduction equation which governs heat flow through the wall is given by,

$$\rho C \frac{dT}{dt} = -\frac{1}{x^m}\frac{d(x^m q_x)}{dx} \tag{6.2}$$

where

$$q_x = -k\frac{\partial T}{\partial x} \tag{6.3}$$

and ρ, C and k are the wall density, heat capacity and thermal conductivity respectively. The exponent $m = 0$ for a planar wall, $m = 1$ for a cylindrical wall and $m = 2$ for a spherical wall. x represents the spatial coordinate along which the one-dimensional heat conduction takes place with $x = 0$ corresponding to the interior wall adjacent to the gas mixture and $x = L$ representing the outer surface of the wall adjacent to the ambient. The wall thickness L is specified by the user.

Figure 5 illustrates the finite difference discretization through the wall thickness. The wall thickness is spatially divided into $N_{max} - 1$ segments each having a thickness of Δx. The number of segments into which the wall is divided is specified by the user. The locations $x_1, x_2, x_3, \ldots, x_{N-1}, x_N, x_{N+1}, \ldots, x_{NMAX-1}, x_{NMAX}$ are places where wall temperatures will be calculated. The temperatures making up the wall temperature distribution are T_1 through T_{NMAX}. The temperature T_1 is the interior wall temperature adjacent to the gas mixture and T_{NMAX} is the exterior wall temperature adjacent to the ambient. The locations x_n represent the centers of heat conduction control volumes. The boundaries of these control volumes are represented by the vertical dashed lines shown in Figure 5. Each of the control volume boundaries is positioned midway between adjacent x locations, the exceptions being the left boundary of control volume 1 which is position at x_1 and the right boundary of control NMAX which is positioned at x_{NMAX}.

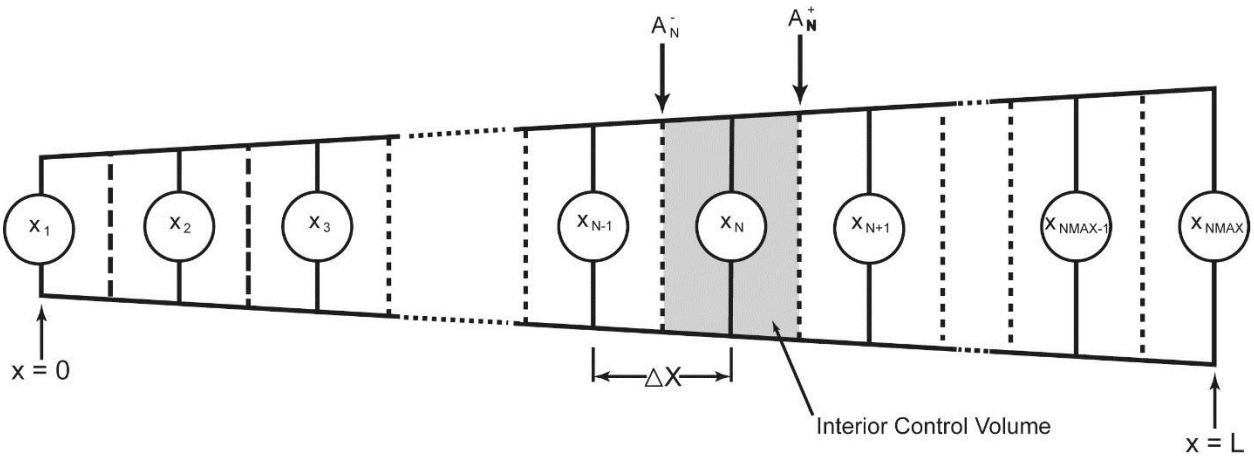

Figure 5. Finite difference grid for one-dimensional heat conduction through the wall.

Wall Interior Temperatures

Figure 5 is drawn to emphasize the fact that the volume of each control volume and the surface areas of the control volume interfaces increase through the thickness of the wall. The way these volumes and surface areas increase is dependent on the geometry specified by the user. For a planar wall there is no increase, for a cylindrical wall these quantities increase linearly with x and for a spherical wall these quantities increase with the square of x. NETFLOW automatically calculates the volume of each control volume and the surface areas of the control volume interfaces as part of the finite difference mesh building process.

We can the write transient energy equation for any interior control volume centered at x_n as a finite difference in time, *i.e.*,

$$\rho C V_n \frac{(T_N^{t+\Delta t} - T_N^T)}{\Delta t} = q_N^- - q_N^+ \tag{6.4}$$

where V_N is the volume of the control volume centered at x_N, q_N^- is the heat flow due to conduction at the left boundary of the control volume and q_N^+ is the heat flow due to conduction at the right boundary of the control volume. The quantity T_N^t is the temperature at the current time step t and $T_N^{t+\Delta t}$ is the temperature at the next time step (This is the quantity we wish to explicitly calculate). We can utilize a simple finite difference in space together with Fourier's Law to write expressions for q_N^- and q_n^+,

$$q_N^- = -A_N^- \, \mathrm{k} \left(\frac{T_N^t - T_{N-1}^t}{x_N - x_{N-1}} \right) \tag{6.5}$$

$$q_N^+ = +A_N^+ \, \mathrm{k} \left(\frac{T_{N+1}^t - T_N^t}{x_{N+1} - x_N} \right) \tag{6.6}$$

where A_N^- and A_N^+ are the surface areas of the left and right control volume interfaces.

Substituting Equations (6.5) and (6.6) into Equation (6.4) and solving for $T_N^{t+\Delta t}$ we obtain the following expression for updated temperatures at all interior $(1 < N < NMAX)$ control volumes,

$$T_N^{t+\Delta t} = T_N^T - \frac{A_N^- k \, \Delta t}{\rho_N C_N V_N} \frac{(T_N^t - T_{N-1}^t)}{(x_N - x_{N-1})} + \frac{A_N^+ k \, \Delta t}{\rho_N C_N V_N} \frac{(T_{N+1}^t - T_N^t)}{(x_{N+1} - x_N)} . \tag{6.7}$$

Because the calculation of temperature at the new time set is explicit, the selection of the time step is limited by stability requirements. Given a particular mesh spacing (*i.e.* Δx where $\Delta x = x_N - x_{N-1} = x_{N+1} - x_N$) it can be shown (see *e.g.* Kreith [31]) that for stability, the following criterion must be met:

$$\Delta t \leq \frac{1}{2} \frac{\Delta x^2}{a} \tag{6.8}$$

where *a*, the thermal diffusivity of the wall is defined by:

$$a = \frac{k}{\rho C} . \tag{6.9}$$

In order to specify the temperature at the interior (gas mixture side) and exterior (ambient side) wall, it is necessary to derive two new equations for $T_1^{t+\Delta t}$ and $T_{NMAX}^{t+\Delta t}$. These equations can be derived from simple one-dimensional energy balances as outlined in the next two sub-sections.

Wall Interior Boundary Temperature (Left Boundary)

Figure 6 shows a shaded solid control volume at the interior side of the wall. The left boundary of this control is located at $x = x_1$ and the left boundary is located on a plane equidistant between x_1 and x_2. Heat enters the control volume at left boundary in the form of convective

heat transfer (Newton's Law of Cooling). Heat exits the control volume at the left boundary in the form of heat conduction (Fourier's Law). Hence the transient energy balance for the control volume is

$$\rho CV_1 \frac{T_1^{t+\Delta t} - T_1^t}{\Delta t} = A_1 h(T_{GAS} - T_1^t) + A_1^+ k \frac{(T_2^t - T_1^t)}{x_2 - x_1} \tag{6.10}$$

where T_{GAS} is the temperature of the gas mixture in the node that is adjacent to the interior wall.

Equation (6.10) can be explicitly solved for the new temperature at x_1 *i.e.*,

$$T_1^{t+\Delta t} = T_1^t + \frac{A_1 h \Delta t}{\rho C V_1}(T_{GAS} - T_1^T) + \frac{A_1^+ k \Delta t}{\rho C V_1} \frac{(T_2^t - T_1^t)}{(x_2 - x_1)}. \tag{6.11}$$

Note that $T_1^{t+\Delta t}$ represents the time updated value of T_w in Equation (6.1).

The explicit calculation of $T_1^{t+\Delta t}$ will be stable providing a time step is selected that satisfies the following stability criterion [31]:

$$\Delta t \leq \frac{\Delta x^2}{a}\left(\frac{1}{1 + h\Delta x/k}\right). \tag{6.12}$$

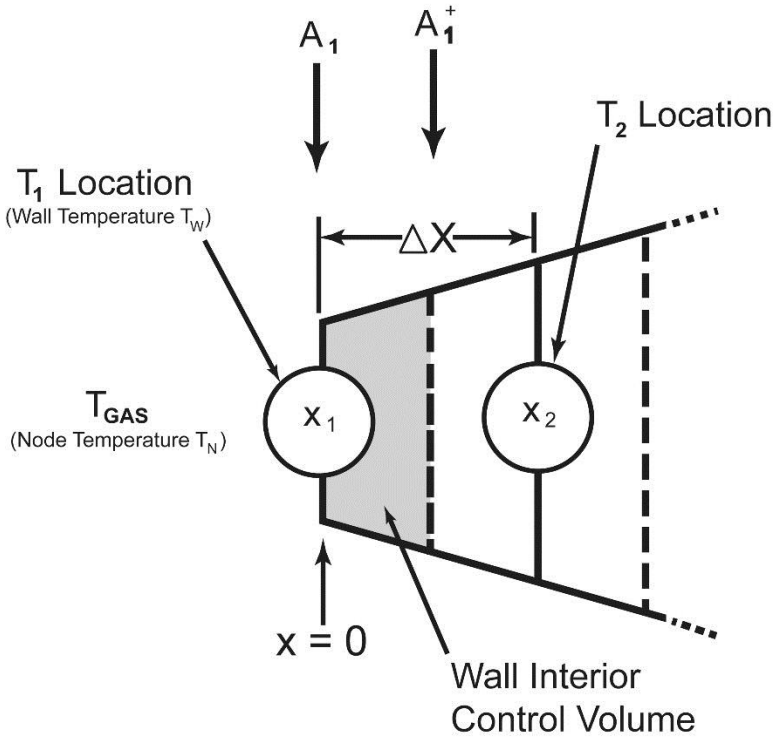

Figure 6. Finite difference grid at the interior wall (Left Boundary Condition).

Wall Exterior Boundary Temperature (Right Boundary)

Figure 7 shows a shaded solid control volume at the exterior side of the wall. The left boundary of this control is located on a plane equidistant between x_{NMAX-1} and x_{Nmax}. Heat enters the control volume at left boundary the form of heat conduction (Fourier's Law. Heat exits the control volume at the right boundary in the form of convective heat transfer (Newton's Law of Cooling) to the ambient. Hence the transient energy balance for the control volume is

$$\rho CV_1 \frac{T_{NMAX}^{t+\Delta t} - T_{1NMAX}^{t}}{\Delta t} = -\bar{A_{NMAX}} k \frac{(T_{NMAX}^{t} - T_{NMAX-1}^{t})}{(x_{NMAX} - x_{Nmax-1})} - \mathrm{A}_{NMAX} h_{AMB} (T_1^t - T_{AMB}) \quad (6.13)$$

where T_{AMB} is the ambient temperature and h_{AMB} is the convective heat transfer coefficient for heat transfer to the ambient.

Equation (6.13) can be explicitly solved for the new temperature at x_{NMAX} *i.e.*,

$$T_{NMAX}^{t+\Delta t} = T_{NMAX}^{t} - \frac{\bar{A_{NMAX}} k \Delta t}{\rho CV_{NMAX}} \frac{(T_{NMAX}^{t} - T_{NMAX}^{t})}{(x_{NMAX} - x_{NMAX-1})} - \frac{A_{NMAX} h \Delta t}{\rho C V_{NMAX}} (T_{NMAX}^{T} - T_{AMB}) \quad (6.13)$$

The explicit calculation of $T_{NMAX}^{t+\Delta t}$ will be stable providing a time step is selected that satisfies the following stability criterion [31]:

$$\Delta t \leq \frac{\Delta x^2}{a} \left(\frac{1}{1 + h_{AMB} \Delta x / k} \right). \quad (6.14)$$

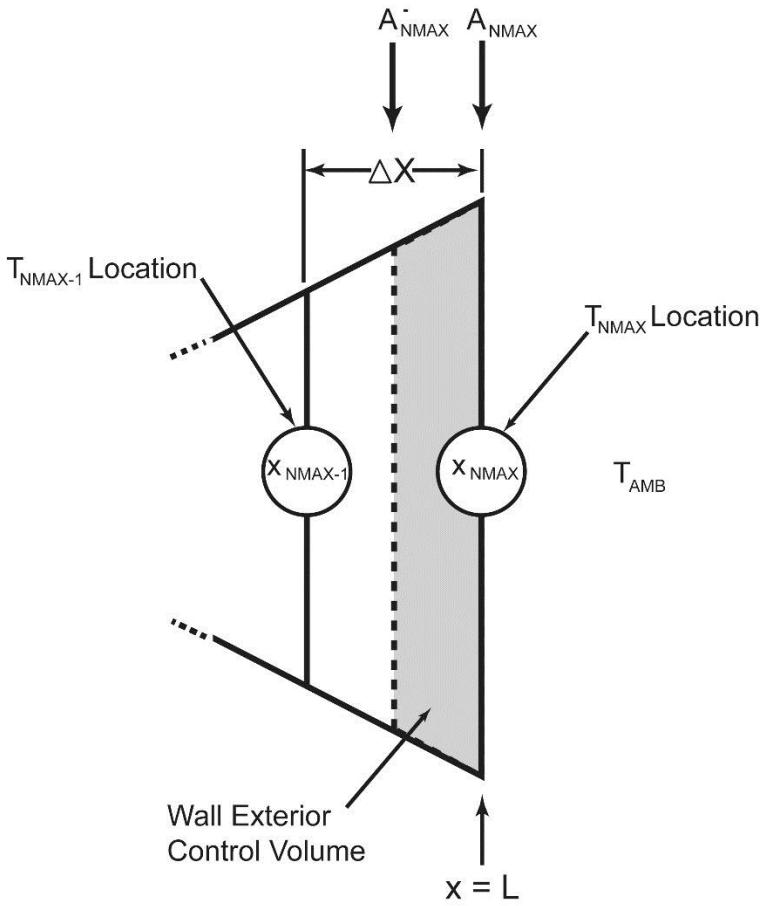

Figure 7. Finite difference grid at the exterior wall (Right Boundary Condition).

In Summary

Each time NETFLOW prints results to the output files it calculates a new set of wall temperatures using Equations (6,11), (6.6) and (6.13). The time step, Δt, used in the explicit calculation of this temperature field is the largest time step that satisfies all three stability criteria defined by Equations (6.7), (6.12) and (6.14). If the print interval is smaller than the stable explicit time step, Δt is set to the print interval and only one time step is taken. If the print interval is larger than the stable explicit time step (This is usually the case.), a series of explicit time steps is taken to advance the heat conduction solution to the time at which NETFLOW output is printed.

REFERENCES

[1] W. S. Winters, "A New Approach to Modeling Fluid/Gas Flows in Networks," Sandia Technical Report SAND2001-8422, Sandia National Laboratories, Livermore, CA, July 2001.

[2] W. S. Winters, C. E. Hickox, G.E. EVANS, M. J. Martinez, B. M. Rush, D. K. Gartling, G. F. Homicz, and J. S. Grieco, "Detailed Modeling and Simulation of Contaminant Transport in Architectural Spaces – Final Report: LDRD Project No. 52711," Sandia Technical Report SAND2005-7465, Sandia National Laboratories, Livermore, CA, September 2005.

[3] V. H. Ransom and R. R. Wagner, "RELAP5/Mod1 Code Manual Volume 1: System Models and Numerical Methods," NUREG/CR-1826, EG&G Idaho, Inc., Idaho Falls, ID, March 1981.

[4] RETRAN-02—A program for Transient Thermal-Hydraulic Analysis of Complex Fluid Flow Systems, Volume 1 Equations and Numerics," Technical Report NP-1850-CCM, Energy Incorporated, P.O, Box 736, 1 Energy Drive, Idaho Falls, Idaho, 1981.

[5] L. F. Moody, "Friction Factors for Pipe Flow," *Transactions of the ASME*, Volume 66, No. 8, p. 671, 1944.

[6] W. S. Winters, "TOPAZ-A Computer Code for Modeling Heat Transfer and Fluid Flow in Arbitrary Networks of Pipes, Flow Branches and Vessels," Sandia Technical Report SAND83-8253, Sandia National Laboratories, Livermore, CA, January 1984.

[7] W. S. Winters, "TOPAZ-The Transient One-Dimensional Pipe Flow Analyzer: User's Manual," Sandia Technical Report SAND85-8251, Sandia National Laboratories, Livermore, CA, July 1985.

[8] W. S. Winters, "TOPAZ- The Transient One-Dimensional Pipe Flow Analyzer: Code Validation and Sample Problems," Sandia Technical Report SAND85-8236, Sandia National Laboratories, Livermore, CA, October 1985.

[9] W. S. Winters, "TOPAZ- The Transient One-Dimensional Pipe Flow Analyzer: Equations and Numerics," Sandia Technical Report SAND85-8248, Sandia National Laboratories, Livermore, CA, December 1985.

[10] W. S. Winters, "TOPAZ- The Transient One-Dimensional Pipe Flow Analyzer: An Update on Code Improvements and Increased Capabilities," Sandia Technical Report SAND87-8225, Sandia National Laboratories, Livermore, CA, September 1987

[11] L. R. Petzold, "A Description of DASSL: A Differential/Algebraic System Solver," Sandia Technical Report SAND82-8637, Sandia National Laboratories, Livermore, CA, September 1982.

[12] L. R. Petzold, P. N. Brown, A. C. Hindmarsh, and C. W. Ulrich "DDASKR-Differential Algebraic Solver Software," Center for Computational Science & Engineering, L-316, Lawrence Livermore National Laboratory, P. O. Box 808, a private communication with L. R. Petzold.

[13] S. V. Patankar, Numerical Heat Transfer and Fluid Flow, Hemisphere Publishing Company, 1980.

[14] R. D. Blevins, *Applied Fluid Dynamics Handbook*, Van Nostrand Reinhold Company Inc., New York, NY, 1984.

[15] *Flow of Fluids Through Valves, Fittings and Pipe*, Technical Paper No. 410, Crane Company, New York, NY, 1980.

[16] A. H. Shapiro, The Dynamics and Thermodynamics of Compressible Fluid Flow, Volume 1, p. 76, John Wiley & Sons, New York, NY, 1953,

[17] Bird, R. B., Stewart, W. E., and Lightfoot, E. N., *Transport Phenomena*, John Wiley & Sons, Inc., pp. 471-473, 1960.

[18] A. Shugard and P. Van Blarigan, "Characteristics of Gas Flow in a Porous Media Compact," Sandia Technical Report SAND2006-6160, Sandia National Laboratories, Livermore, CA, October 2006.

[19] W. S. Winters, "Implementation and Validation of the NETFLOW Porous Media Model," Sandia Technical Report SAND2009-6838, Sandia National Laboratories, Livermore, CA, December 2009.

[20] Private communication with B. L. Bon, Department 8254, 2012.

[21] D. R. Chenoweth, "Gas-Transfer Analysis Section H-Real Gas Results vis the van der Waals Equation of Stane and Virial Expansion Extensions of its Limiting Abel-Nobel Form," Sandia Technical Report SAND83-8229, Sandia National Laboratories, Livermore, CA, June 1983.

[22] G. J. Van Wylen and R. E. Sonntag, Fundamentals of Classical Thermodynamics-SI Version 2^{e}, John Wiley and Sons, Inc., New York, NY, 1976.

[23] R. H. Sabersky and A. J. Acosta, Fluid Flow – A First Course in Fluid Mechanics, Macmillan Company, New York, p. 216, 1964.

[24] C. F. Colebrook and C. M. White, *Journal of the Institute of Civil Engineering*, Volume 10, No. 1, pp 99-118, 1939.

[25] S. W. Churchill, *Chemical Engineering*, pp 91-92, November 1977.

[26] F. W. Dittus and L. M. K. Boelter, University of California (Berkeley) *Pub. Eng.*, Volume 2 p. 443, 1930.

[27] W. S. Winters, G. H. Evans, S. F. Rice and R. Greif, "An Experimental an Theoretical Study of Heat and Mass Transfer during the Venting of Gas from Pressure Vessels," International Journal of Heat and Mass Transfer, Volume 55, pp 8-18, 2012

[28] W. S. Winters, G. H. Evans, S. F. Rice, N. J. Paradiso, T. G. Felver, "Transient PVT Measurements and Model Predictions for Vessel Heat Transfer –Part II," Sandia Technical Report SAND2010-4683, Sandia National Laboratories, Livermore, CA, July 1985.

[29] G. L. Clark, "A Zero-Dimensional Model for Compressible Gas Flow in Networks of Pressure Vessels-Program TRIC." Sandia Technical Report SAND83-8226, Sandia National Laboratories, Livermore, CA, July 1983.

[30] J. D. Means and R. D. Ulrich, "Transient Convective Heat Transfer During and After Gas Injection into Containers," *Journal of Heat Transfer*, pp 282-287, May 1975.

[31] F. Kreith, Principles of Heat Transfer, Third Edition, Harper & Row Publishers, New York, NY 1973.

[32] E. W. Lemmon, M. L. Huber and M. O. McLinden, NIST Reference Fluid Thermodynamic and Transport Properties—REFPROP, Version 8 User's Guide, April 2007.

APPENDIX A – ISENTROPIC FLOW AT RESERVOIR EXITS

In some cases it is desirable to use an isentropic flow path to simulate the flow from the stagnation point in a reservoir to the high speed flow point in the exit tubing. As an example, consider the Transient PVT Experiments conducted by Rice *et. al.* [27-28]. Their experimental apparatus consisted of a reservoir, a receiver and a single interconnecting flow path that began with an orifice connected to a series of much larger diameter tubes. The orifice attached to the reservoir was designed to have a smooth and rounded transition from the reservoir to the orifice diameter. This transition minimized the form loss that would normally result from a "sharp edged" transition. The plumbing between the reservoir and the receiver was designed so that virtually all pressure drop between the reservoir and the receiver was across the orifice. *(i.e.* there was insignificant pressure drop in the tubing between the orifice and the receiver.

Attempts to simulate the reservoir/receiver transfers in Rice's experiments were made using NETFLOW, However whenever the standard tube model as represented by the mixture momentum Equation (2.6) was used, an over prediction of the time required for the transfer resulted. The standard tubing model makes the assumption that the flow transition is "sharp-edged" and as such a form loss factor, K_A will be applied to account for the area change between the reservoir diameter and the orifice diameter. The value of the form loss is apparent from the first term on the right hand side of Equation (2.8). For most very large to very small area transitions the form loss approaches 0.5 meaning there is half a dynamic head loss term in the momentum equation which serves to slow the flow. The influence of the area change form loss may be negated by applying a zero area form loss multiplier for the flow path. This may be done using the directive "KAMULT=0" in describing the flow path. (See the description of the PATH directives in APPENDIX A). However the transfer time will still be over predicted (although by a lesser amount) because the finite difference form of the momentum equation will not replicate isentropic flow, even if there are no pressure loss terms to retard the flow.

To illustrate these points further, a series of NETFLOW calculations were performed to simulate the system shown in Figure B-1. The system consists of a 200 cc reservoir and a 700 cc receiver connected by a constant diameter (0.060 inches) flow path. The first portion of the flow path is attached to the receiver. This flow path is extremely short (0.0001 inches) and as such has a negligible friction pressure loss. The second part of the flow path consists of a tube which is either 1 inch long (small frictional pressure drop) and 100 inches long (large frictional pressure drop).

A series of six NETFLOW calculations were made, three with the 1 inch tube and three with the 100 inch tube. Helium was used as the transfer gas and the standard Moody tube flow friction model was used. Heat transfer in the reservoir and receiver was simulated with the "Combined" model. The results are illustrated in Figure B-2 which shows the pressure decay in the reservoir for each calculation.

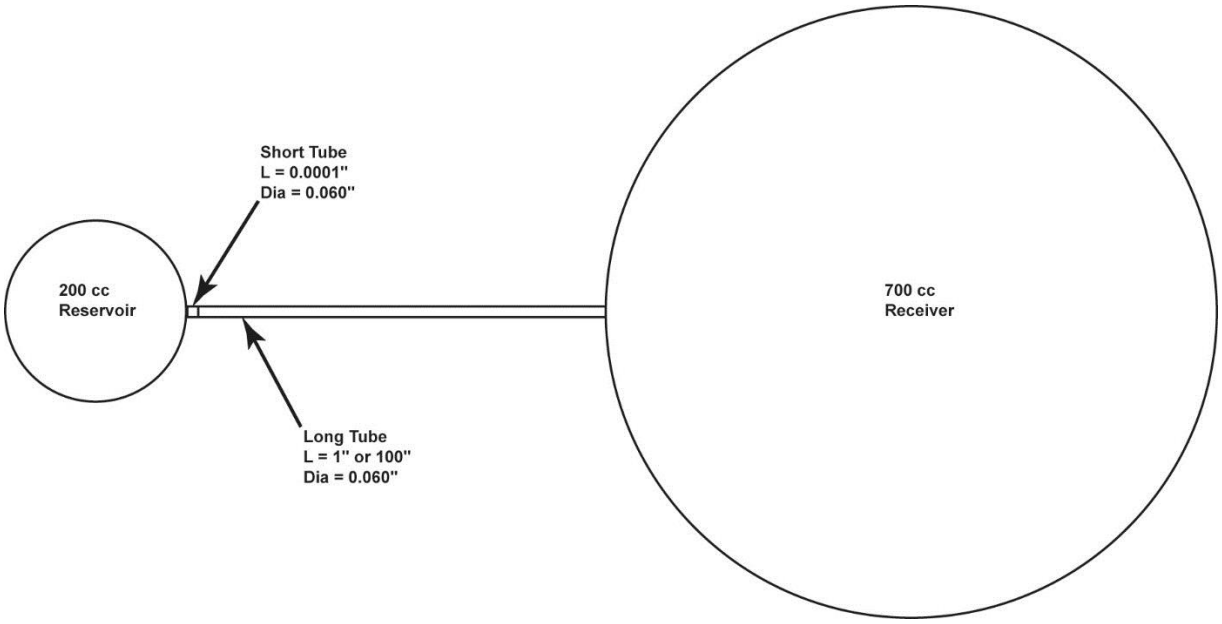

Figure B-1 Schematic of the network flow system.

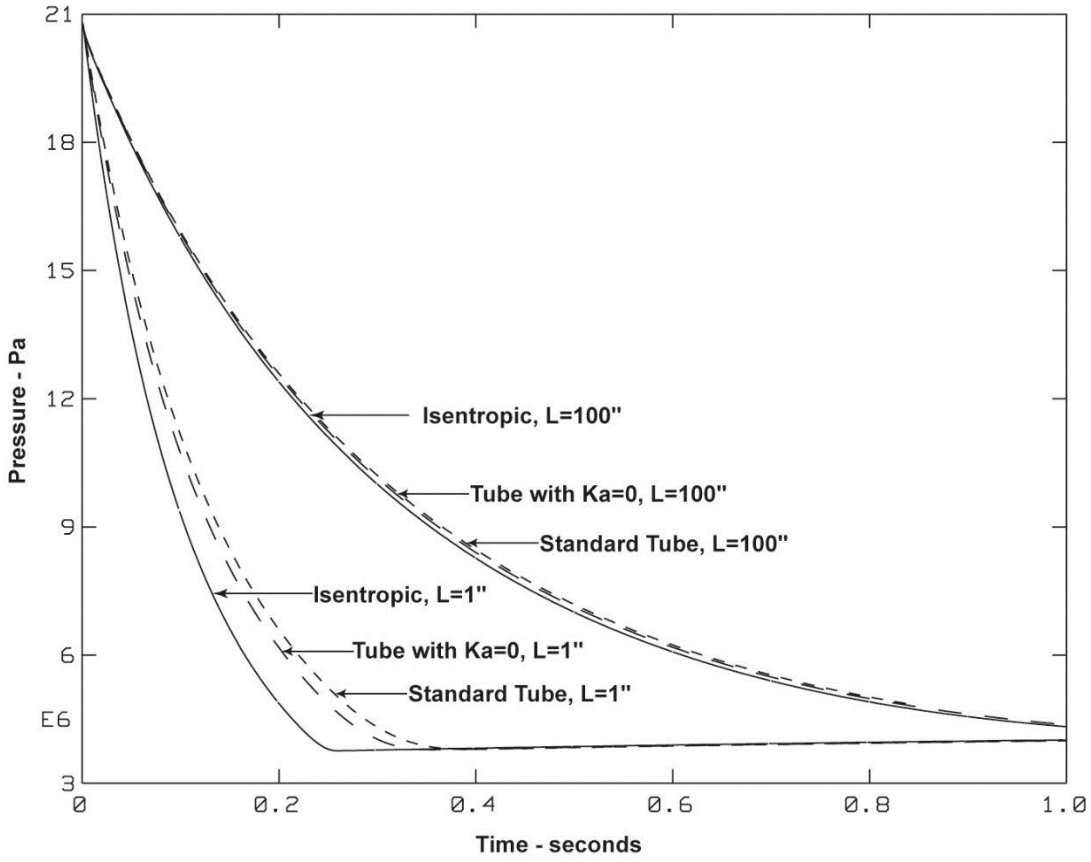

Figure B-2 Reservoir blowdown transients.

The three curves on the left in Figure B-2 represent reservoir pressure transients that resulted from using a 1 inch tube as the "long tube". The solid line is the result using the isentropic model for the short tube. This was fastest transfer. The short dashed lined is the result using the standard tube model with area form loss for the short tube. This was the longest transfer. A slightly shorter transfer results if the standard tube model is used without the area form loss (long dashed line), however even this model results in a transfer time that is approximately 20% longer that the isentropic model. Hence for systems having small pressure drops (in this case a 1 inch tube), significant errors could occur as a result by modeling a truly isentropic reservoir transition with non-isentropic model.

The three curves on the right in Figure B-2 represent reservoir pressure transients that resulted from using a 100 inch tube as the "long tube" Once again the solid line is the isentropic result, the short dashed line is the standard tube result with area form loss and the long dashed line in the standard tube result without area form loss. The qualitative results in the speed of transfer persist in that the fastest pressure decay occurs with the isentropic model and the slowest pressure decay occurs with the standard tube model with area form loss. However, the quantitative differences in the three short tube models are negligible. Hence in systems having large pressure drops modeling a truly isentropic reservoir transition with a non-isentropic model will not lead to large errors in predicting transfer times.

APPENDIX B – PROCEDURE FOR COMPUTING THE ABEL-NOBLE MIXTURE PARAMETER

A unique co-volume constant exists for each species in the Abel-Noble mixture model. Section 3.0 lists constants for the hydrogen and helium isotopes. Constants for other species can be obtained by comparing PVT characteristics of the Abel-Noble equation of state (Equations 3.6 and 3.7) to actual data or to more complete models such as REFPROP [32]. The present authors have done this for Xe, CO_2 and Ar.

In order to complete the thermodynamics for the Abel-Noble Mixture model it is necessary to develop a means to determine a combined co-volume mixture constant for the mixture. This is accomplished by extending the method suggested by Chenoweth [21] for binary Able-Noble mixtures.

The combining rule utilizes molar values of the species co-volume constants (i.e. units for b are converted from m^3/kg to m^3/kg-mole) and the mole fractions of each species in the mixture.

For a single species mixture the mixture co-volume constant is given by

$$\bar{b}_{MIX} = \bar{b}_1 \tag{C-1}$$

where $\bar{b}_{MIX}$ is the mixture molar co-volume constant and $\bar{b}_1$ is the species molar co-volume constant.

For a binary mixture the mixture co-volume constant is given by

$$\bar{b}_{MIX} = X_1\bar{b}_1 + X_2\bar{b}_2 + 0.5X_1\bar{b}_1\left(\frac{X_2\bar{b}_2}{\bar{b}_1+\bar{b}_2}\right) \tag{C-2}$$

where X_1 and X_2 are the mole fractions for each species.

For a trinary mixture the mixture co-volume constant is given by

$$\bar{b}_{MIX} = X_1\bar{b}_1 + X_2\bar{b}_2 + X_3\bar{b}_3 + 0.5X_1\bar{b}_1\left(\frac{X_2\bar{b}_2}{\bar{b}_1+\bar{b}_2}\right)$$

$$+0.5X_2\bar{b}_2\left(\frac{X_2\bar{b}_2}{\bar{b}_1+\bar{b}_2} + \frac{X_3\bar{b}_3}{\bar{b}_2+\bar{b}_3}\right) \tag{C-3}$$

For a mixture containing more than three species the series suggested above is extended using the usual FORTRAN 95 do loop constructs.

Once the mixture molar co-volume constant is obtained, it is converted to a mass-massed constant using the mixture molecular weight, *i.e.*

$$b_{MIX} = \bar{b}_{MIX}\,/MW_{MIX} \tag{C-4}$$

APPENDIX C – IMPACT OF CONSTANT TEMPERATURE PROPERTIES

In order to determine the importance of temperature dependent properties for the specific heats and transport properties, a new version of the Abel-Noble mixture model was developed. This newer version can be invoked by the user through the command MIXTURE=TABELNOBLE (or MIXT=TABE in short form).

When this model is used the specific heats and transport properties for each species are temperature dependent. Each property is then expressed in terms of a polynomial in temperature, T. Each polynomial was fitted to REFPROP [32] predictions for the properties C_v , C_p, k and μ. The internal energy of gas mixture was determined from its definition

$$du(T) = C_v(T)dT \tag{D-1}$$

by integrating over temperature, noting that u is defined to be zero when T is zero. Hence,

$$u(T) = \int_0^T C_v(T)dT\ . \tag{D-2}$$

In order to implement the TABELNOBLE model, it was necessary to reformulate the transient term in the mixture energy Equation (2.3). Using chain rule differentiation the transient term in the mixture energy equation can be rewritten as

$$\frac{d}{dt}[E_N] = \frac{d}{dt}\left[M_N\left(u_N + \frac{V_N^2}{2}\right)\right] = \left(u_N + \frac{V_N^2}{2}\right)\frac{dM_N}{dt} + M_N C_{vN}\frac{dT_N}{dt} + M_N v_N \frac{dv_N}{dt}, \tag{D-3}$$

Hence the transient energy term has three parts. The DASKR dependent variable E_N is now replaced by T_N in Equation (5.6). The derivative $\frac{dM_N}{dt}$ is determined from Equations (2.1) and (2.2). The derivative $\frac{dv_N}{dt}$ is obtained from the time derivative of the nodal mass flow rate, *i.e.*,

$$\dot{W}_N = \frac{d}{dt}(\rho_N A_N v_N). \tag{D-3}$$

By carrying out chain-rule differentiation on the right hand side of Equation (D-3) and solving for $\frac{dv_N}{dt}$ the following expression is obtained:

$$\frac{dv_N}{dt} = \frac{W_N}{\rho_N A_N} - \frac{v_N}{\rho_N V_n}\frac{dM_N}{dt} \tag{D-4}$$

where $\frac{dM_N}{dt}$ is once again determined from Equations (2.1) and (2.2) and $\dot{W}_N$ is determined from the time derivative of Equation (2.5).

In order to compare the default ABELNOBLE mixture model (constant properties for specific heats and transport properties) to the new TABELNOBLE mixture model (temperature

dependent properties for specific heats and transport properties), a NETFLOW simulation was devised in which a reservoir containing a 50:50 mixture (by mass) of hydrogen and deuterium was vented to atmosphere. Hydrogen and deuterium were selected since their specific heats are temperature dependent.

Figure D-1 compares reservoir temperatures computed by the ABELNOBLE and TABLENOBLE mixture models during the adiabatic blowdown to atmospheric pressure. The final temperatures achieved by the ABELNOBLE and TABELNOBLE models were 103.8 K and 97.9 K respectively. The corresponding residual masses computed by the ABELNOBLE and TABLENOBLE models were .0642 g and .0681 g respectively. Figure D-2 shows the mass inventory in the reservoir during the adiabatic blowdown.

Since the reservoir blowdown was adiabatic and wall friction does not play a role in the simulation, the transport properties played no role in causing the differences in computed temperature and mass. These differences are solely due to the temperature dependency of the specific heat as shown in Equation (D-2). While the deviation in the residual reservoir masses is approximately 5.7%, the deviation in the total mass delivered by the reservoir was a negligible 0.2%.

The influences of temperature dependent transport properties can be demonstrated by repeating the simulated blowdown with reservoir heat transfer instead of adiabatic reservoir walls. The head transfer model used was natural convection heat transfer model expressed by Equations (4.8-4.11). Figure D-3 compares reservoir temperatures computed by the ABELNOBLE and TABLENOBLE models. The maximum temperature excursion was approximately 240 K before wall heat transfer causes the reservoir temperature to recover to the initial wall temperature of 423 K. The differences in the computed temperatures for the two models are due to both temperature dependent specific heats and temperature dependent transport properties. The transport properties (μ and k) influence the calculation if the Rayleigh number in Equation (4.11) and thus influence the calculation of the wall heat transfer. Despite a maximum difference in computed reservoir temperature of 15 K at 0.6 seconds, the computed reservoir mass and the total mass delivered is relatively unaffected. This is demonstrated in Figure D-4. The residual mass computed by the ABELNOBLE and TABELNOBLE models was 0.0157862 g and 0.0157852 g respectively.

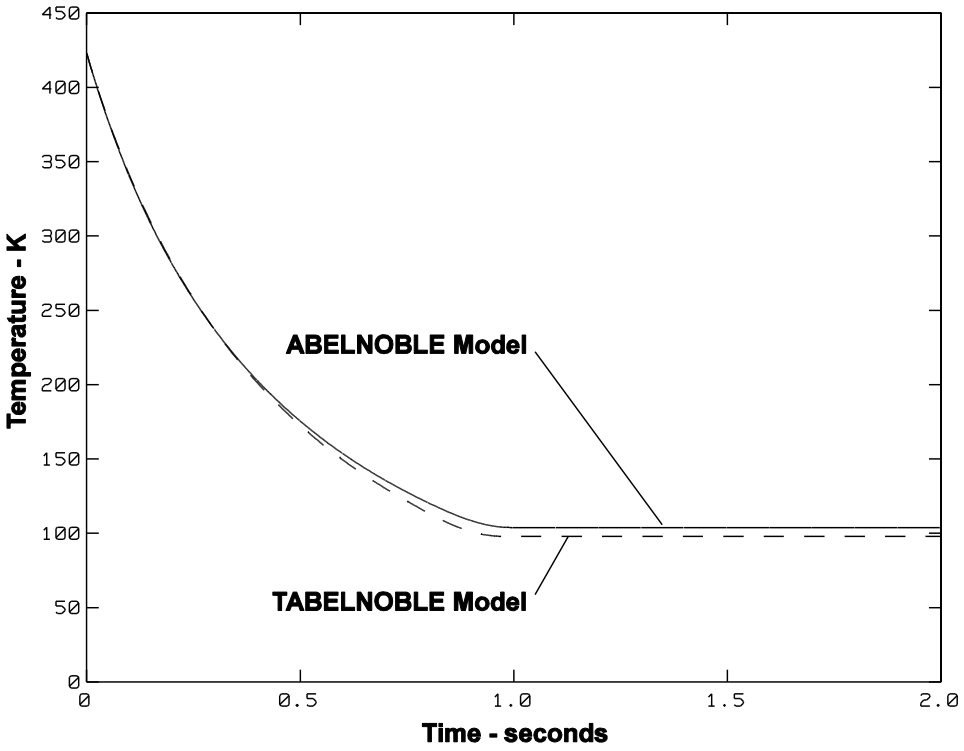

Figure D-1 Reservoir blowdown temperatures for an adiabatic reservoir.

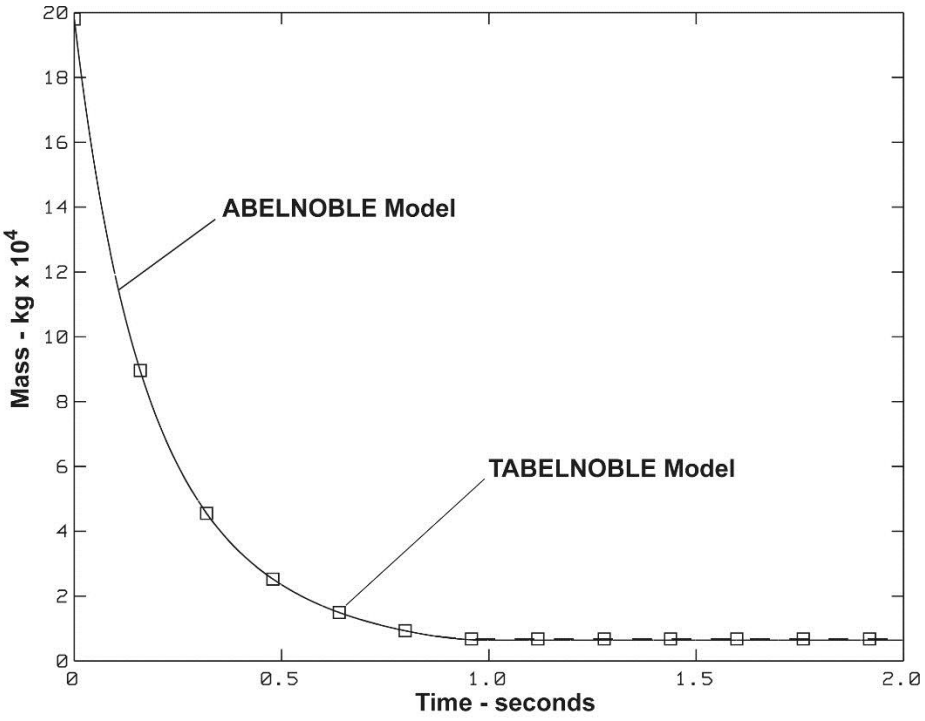

Figure D-2 Reservoir blowdown masses for an adiabatic reservoir.

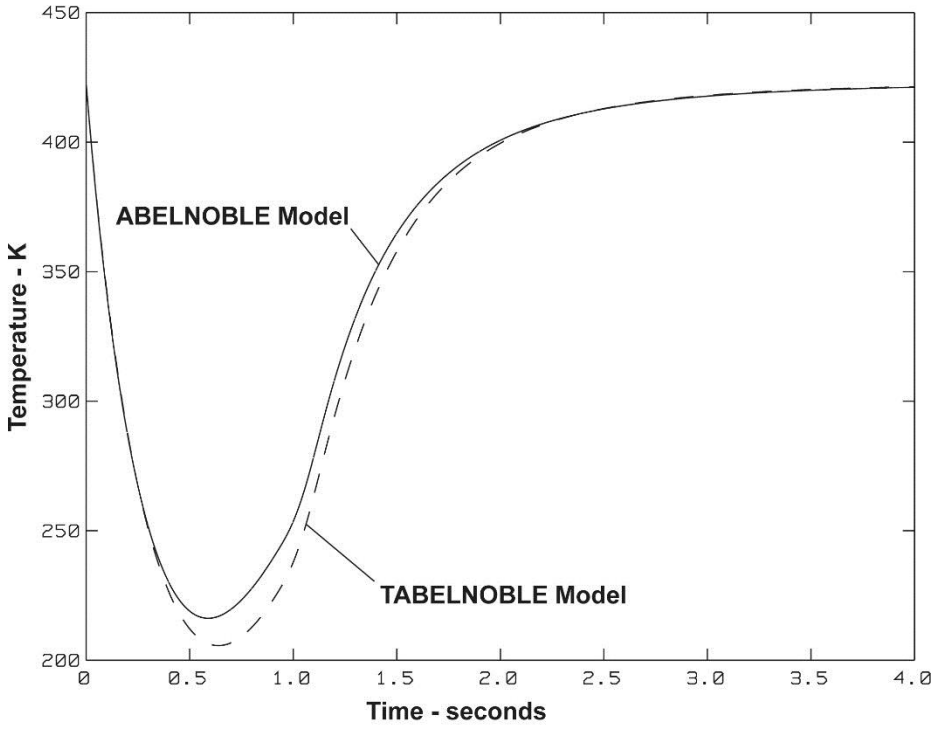

Figure D-3 Reservoir blowdown temperatures with wall heat transfer.

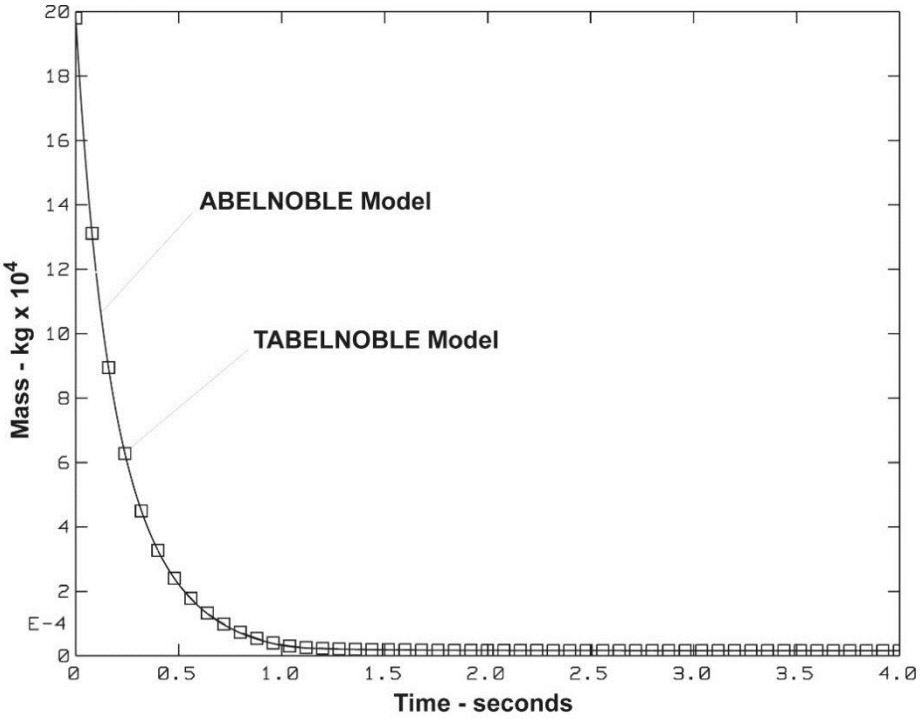

Figure D-4 Reservoir blowdown masses with wall heat transfer.

Several points are worth mentioning with regard to the TABLENOBLE model. The model seems to have little value in improving the computed mass transported from high pressure reservoirs even when those reservoirs undergo wide variations in temperature. The TABELNOBLE model is a more complex mixture model, and computational times typically are increased by a factor of 3 when compared to the ABELNOBLE model. Finally, if the intention is to use the TABLENOBLE model, it should be recognized that heat transfer and pressure drop correlations that were originally developed with experimental data and calculations using constant specific heats and transport properties, would have to be rederived using the temperature dependent mixture model. For example, the leading coefficients of 0.8221 and 0.168 in Equations (4.9) and (4.10) which were obtained using experimental data and computer optimization with multiple NETFLOW ABELNOBLE calculations would need to be rederived using NETFLOW TABLENOBLE calculations.

APPENDIX D – VERIFICATION OF THE WALL HEAT CONDUCTION MODEL

The transient temperature distribution in a Netflow simulation is compared to the analytical solution at various Biot numbers. The comparison is made possible by treating the wall as a single layer plane wall of length 2L that is immersed in a fluid with constant convective heat transfer and constant gas temperature. This was accomplished in NETFLOW by holding a node gas temperature at a constant value and setting Tinf in the wall directive to the same temperature. Hinf and Hgas were also set to the same constant values. Describing the wall as "PLANAR" in the wall directive allowed us to isolate the heat equation in NETFLOW so as to allow for a direct comparison.

There are 4 cases that were tested had the following Biot and heat transfer coefficients:

Bi = 0.010; h = 0.0301 (W/m^2/K)
Bi = 1.000; h = 30.100 (W/m^2/K)
Bi = 10.00; h = 301.00 (W/m^2/K)
Bi = 100.0; h = 3010.0 (W/m^2/K)

The case domain contains three volumes and are defined in NETFLOW as follows:

NODE1 - PATH1 - NODE2 - PATH2 - NODE3

NODE1 and NODE3 are tanks of infinite size. NODE1 has an initial pressure and gas temperature of 1000psi and 500K, respectively. The volume was made infinitely large so the pressure and temperature would remain steady and act as constant boundary conditions. NODE3 was also an infinitely large volume meant to simulate atmosphere. It is initialized the same as NODE2 with Tgas = 300 K and pressure at 1 atm.

NODE2 is the test chamber with a volume of 37 L and a 2 layer wall. Each layer has thickness L and has the exact same wall description. It was initialized to 1 atm, and a gas temp of 500K, and wall temperature of 300 K. A Dirichlet boundary condition was set to keep the gas temperature at a constant 500K. The wall was simulated as a planar geometry with the following parameters:

Interior gas conditions and wall parameters were set as follows:

hg = Specified Above J/s-K-m**2
Tgas = 500 K - Held constant

L = 0.023 (m)
rho = 1577.76 (kg/m^3)
Cp = 1255.8 (J/kg-K)
k = 0.69228 W/m-K

Analytical Solution

Using Heisler charts (see Appendix C in *Heat Transfer* 9th ed. by J.P. Holman) we can approximate the infinite series solutions for the centerline temperature in an planar wall within 1 percent for Fo numbers greater than 0.2.

Transient Temperature Distribution Definitions

$$\Theta_o^* = \frac{\Theta_o}{\Theta_i} = \frac{T_o - T_\infty}{T_i - T_\infty}$$

$$\alpha = \frac{k}{\rho C_p}$$

$$Fo = t^* = \frac{\alpha t}{L^2}$$

$$Bi = \frac{hL}{k}$$

When Fo > 0.2:

The centerline temperature can be approximated using the following:

$$\Theta_o^* \approx C_B \exp(-A_B^2 * Fo)$$

Checking the Fo condition, the solution comparisons are valid after time = 302 seconds.

Infinite Plate

A_B is the solution to:

$$A_B \tan(A_B) = Bi$$

C_B is obtained from:

$$C_B = \frac{4\sin(A_B)}{2A_B + \sin(2A_B)}$$

Solve for Infinite Plate

From Table C-2 in *Heat Transfer* text, the coefficients for the above Heisler solutions are:

Table E-1: Coefficients for Heisler solutions.

Bi #	A_B	C_B
0.01	0.0998	1.0017
1.00	0.8603	1.1191
10.0	1.4289	1.2620
100.0	1.5552	1.2731

Bi = 0.01

This section compares Netflow output to a flat plate transient analytical solution with a Biot number of 0.01. The solution is of the centerline wall temperature defined in Netflow and shows a comparison to the analytical solution with 1% error bars.

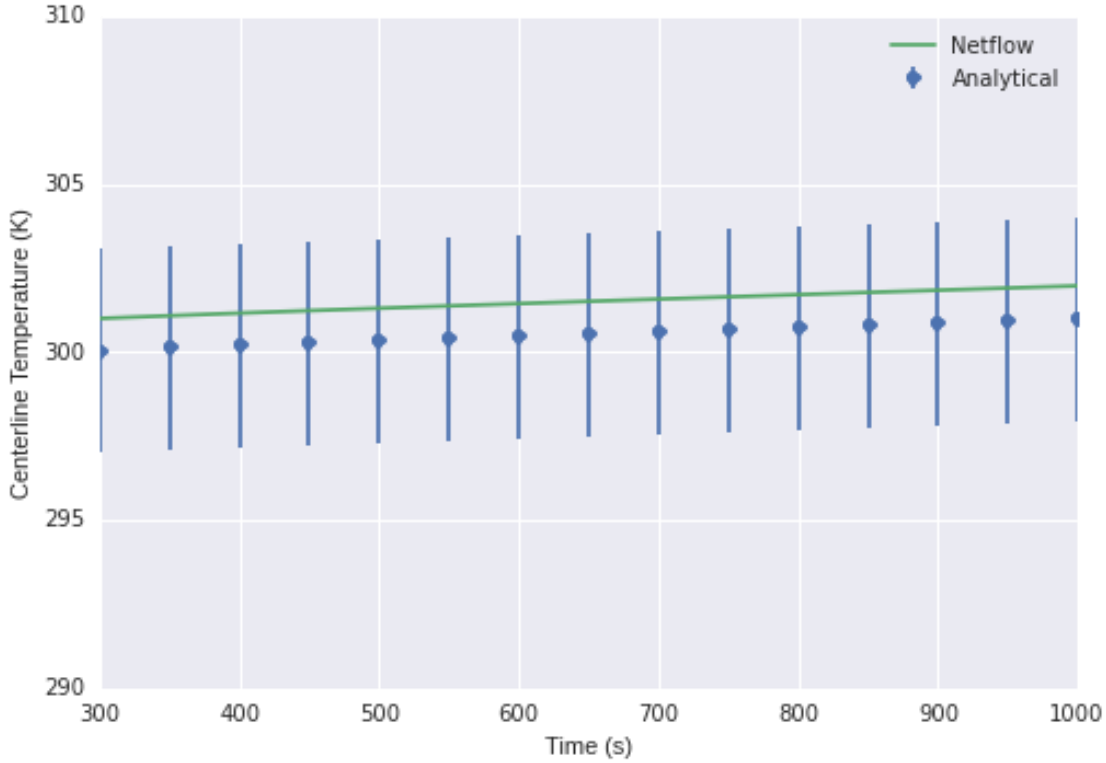

Figure E-1 Transient centerline wall temperature comparison.

Bi = 1.00

This section compares Netflow output to a flat plate transient analytical solution with a Biot number of 1.0. The solution is of the centerline wall temperature defined in Netflow and shows a comparison to the analytical solution with 1% error bars.

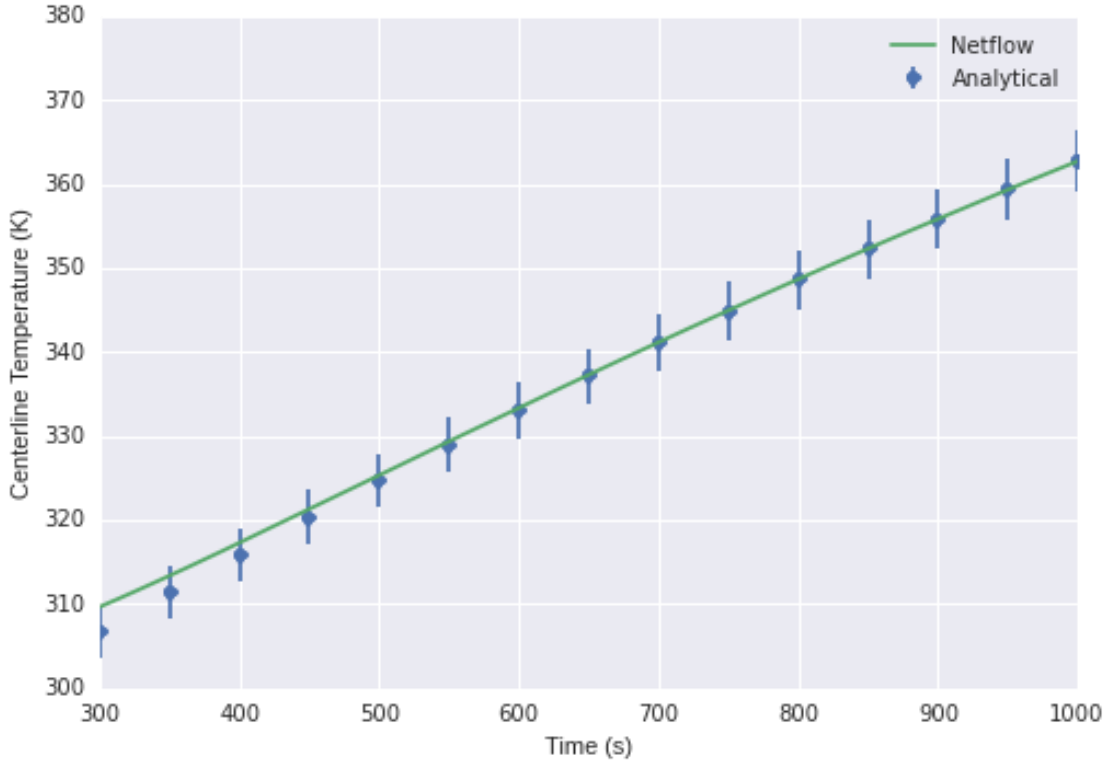

Figure E-2 Transient centerline wall temperature comparison.

Bi = 10.0

This section compares Netflow output to a flat plate transient analytical solution with a Biot number of 10.0. The solution is of the centerline wall temperature defined in Netflow and shows a comparison to the analytical solution with 1% error bars.

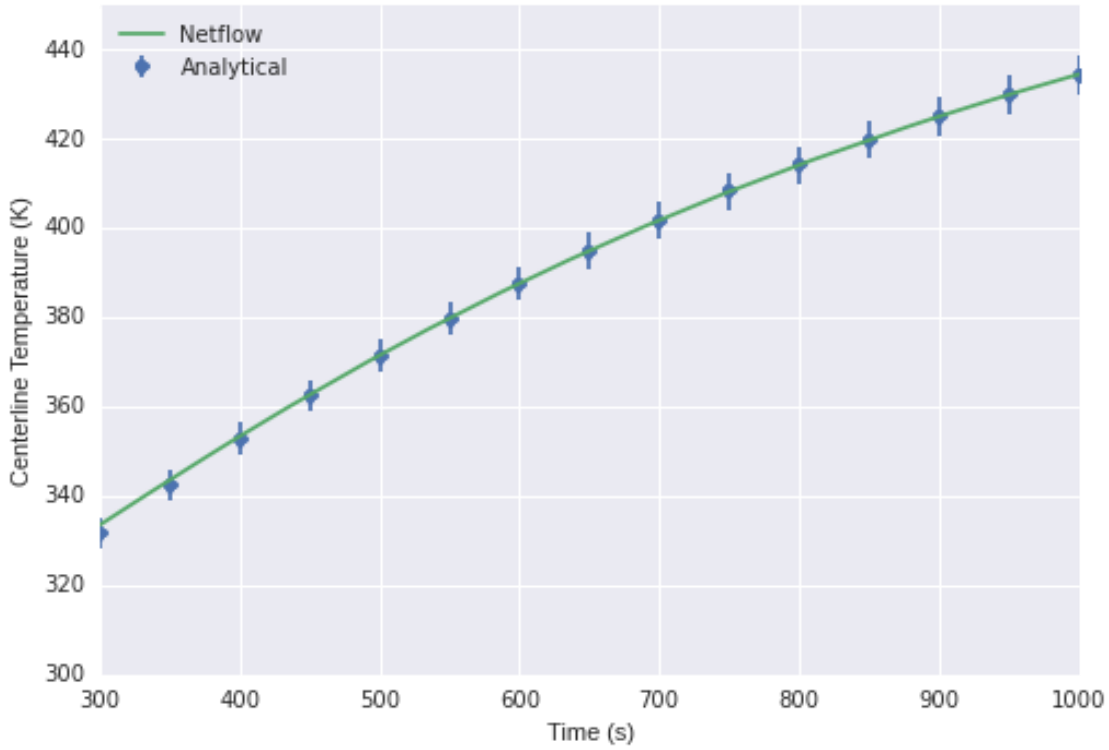

Figure E-3 Transient centerline wall temperature comparison.

Bi = 100.0

This section compares Netflow output to a flat plate transient analytical solution with a Biot number of 100.0. The solution is of the centerline wall temperature defined in Netflow and shows a comparison to the analytical solution with 1% error bars.

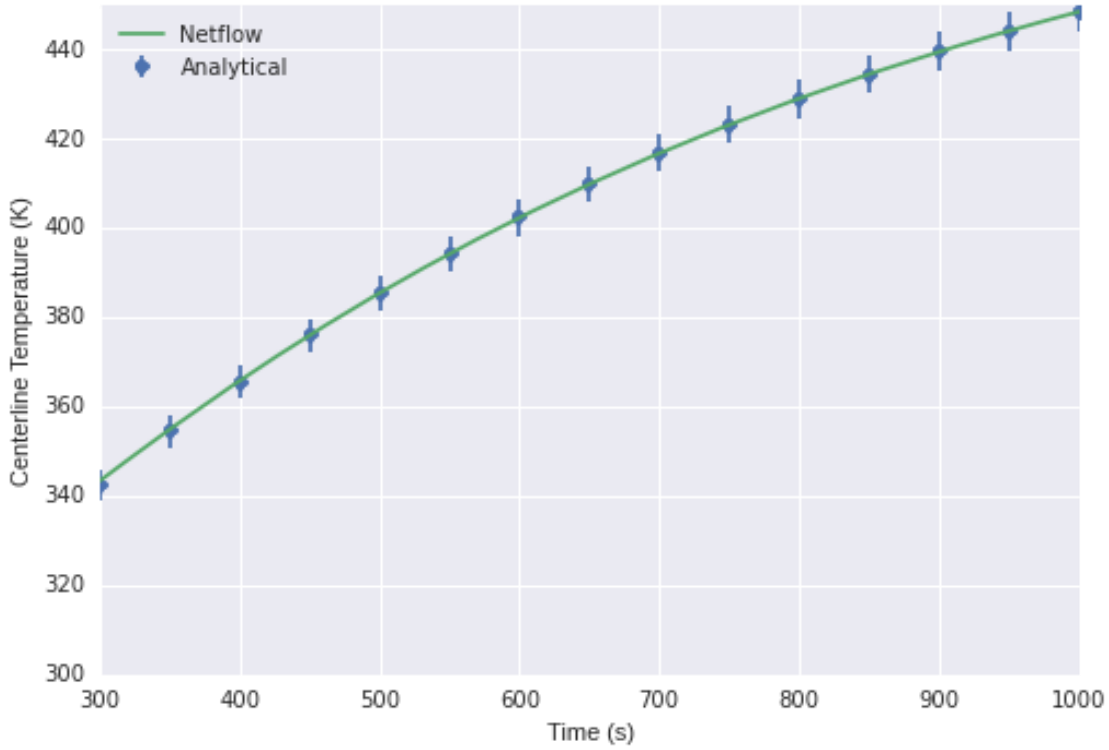

Figure E-4 Transient centerline wall temperature comparison.

DISTRIBUTION

1	MS9035	Brad Bon	Org. 8254
1	MS0899	Technical Library	9536 (electronic copy)


Sandia National Laboratories